


RESEARCH ARTICLE

Recent excavations at Owl Ridge, interior Alaska: Site stratigraphy, chronology, and site formation and implications for late Pleistocene archaeology and peopling of eastern Beringia

Kelly E. Graf¹  | Angela K. Gore¹ | J. Anne Melton² | Tarah Marks³ |
Lyndsay DiPietro⁴ | Ted Goebel¹ | Michael R. Waters¹ | David Rhode⁵

¹Center for the Study of the First Americans, Department of Anthropology, Texas A&M University, College Station, Texas

²Department of Anthropology, University of Minnesota, Minneapolis, Minnesota

³Department of Anthropology, University of Iowa, Iowa City, Iowa

⁴Department of Geology, Baylor University, Waco, Texas

⁵Division of Earth and Ecosystem Sciences, Desert Research Institute, Reno, Nevada

Correspondence

Kelly E. Graf, Center for the Study of the First Americans, Department of Anthropology, Texas A&M University, College Station, TX 77843-4352.

Email: kgraf@tamu.edu

Funding information

Division of Behavioral and Cognitive Sciences and Office of Polar Projects, Grant/Award Numbers: 1029094, 0917648

Scientific Editing by Gary Huckleberry

Abstract

The early archaeological record of Beringia is complicated by the occurrence of several lithic industries. Site assemblages, dating from 14,000 to 12,800 years ago and located from the Yana-Indigirka Lowlands of Siberia to the upper Tanana River basin, contain artifacts characteristic of the Nenana technological complex. After 12,800 years ago, site assemblages contain artifacts diagnostic of the Denali technocomplex. To explain the variation in lithic industries, we first and foremost need well-stratified and well-dated sites with multiple components so we securely know their ages and depositional relationships. We present excavation results of one such site located in interior Alaska, Owl Ridge, with the goal of assessing site stratigraphy, radiocarbon chronology, and natural site formation processes. Owl Ridge was visited three times during the Pleistocene-Holocene transition with a Nenana-complex occupation at 13,380–12,800 years ago followed by two Denali-complex occupations at 12,540–11,430 years ago and 11,270–11,200 years ago. Assemblage change at Owl Ridge was diachronically patterned, as at the nearby Dry Creek archaeological site, and separated by two climatic events, a brief extremely windy Younger Dryas (lasting 300–250 years) and a very brief wetter period (lasting ~160 years). Our results indicate these climate and environmental conditions played a role in settlement of eastern Beringia.

KEYWORDS

Beringia, climate change, Denali complex, Nenana complex, Younger Dryas

1 | INTRODUCTION

The Beringian archaeological record is important when studying the peopling of the Americas because it is via this region that the first Americans traversed (Goebel, Waters, & O'Rourke, 2008; Graf & Buvit, 2017; Potter et al., 2017). Recent genetic models continue to reinforce Beringia as the location where distinctive Native American genetic variability emerged before dispersal into the Western

Hemisphere (Moreno-Mayar, Potter, et al., 2018; Moreno-Mayar, Vinner, et al., 2018; Raghavan et al., 2014). Several archaeological sites with occupations dating to the late Pleistocene, either predating or coeval with Clovis (i.e., older than 13,000 calendar years before present [cal yr BP]), are known from the region (Goebel, Slobodin, & Waters, 2010; Goebel, Waters, & Dikova, 2003; Graf & Bigelow, 2011; Graf et al., 2015; Holmes, 2011; Pitulko et al., 2004; Pitulko, Pavlova, & Nikolskiy, 2017; Potter, Holmes, & Yesner, 2013). To date,

only several of these sites are reported with excavation, stratigraphy, and chronological details required for understanding site formation and placing them in larger models of human behavior and dispersal (e.g., Graf et al., 2015; Pitulko et al., 2004; Potter, Irish, Reuther, Gelvin-Reymiller, & Holliday, 2011; Powers, Guthrie, & Hoffeecker, 2017). Here we add to the emerging Beringian record by reporting excavation results from recent work at Owl Ridge, a multicomponent site located in interior Alaska with layers dating to the late Pleistocene and early Holocene.

1.1 | Background—Research contexts

From the archaeological record of Beringia, we see a complicated array of lithic technologies dating to the late Pleistocene (Goebel & Buvit, 2011a, 2011b). Most of these are unique to Beringia or appear more similar to the Upper Paleolithic technologies found in Northeast Asia than they do to Clovis and contemporary technologies south of the ice sheets (Gómez Coutouly, 2012; but see Goebel, Powers, & Bigelow, 1991). Some Beringian site assemblages contain an industry (here we use the terms “industry” and “technological complex” interchangeably) based on microblade and burin technology with the production of microblade-osseous composite tools and lanceolate bifacial points. These assemblages typically date to the Younger Dryas climatic interval (12,800–11,700 cal yr BP, Hua et al., 2009) and are assigned to the Denali technological complex (Graf & Bigelow, 2011; Hoffeecker, Powers, & Goebel, 1993; Powers and Hoffeecker 1989; Potter et al., 2011), following West (1967). The sites of Swan Point (interior Alaska) and Urez-22 (Yana-Indigirka Lowlands, Russia) also contain microblade technology; however, these site occupations date to 14,400–14,200 cal yr BP and are more reminiscent of the Siberian late Upper Paleolithic Diuktai industry than the later Denali complex (Gómez Coutouly, 2012). For the intervening 1,400 years, following Diuktai and before the appearance of the Denali complex, Beringian site assemblages from the Yana-Indigirka Lowlands to the upper Yukon drainage completely lack microblade technology as well as the lanceolate points of the Denali complex. Instead, they contain small triangular and teardrop-shaped bifacial points (sometimes referred to as “Chindadn”) made on flake blanks, including the small stemmed points from Ushki Lake, and unifacial tools such as end-scrapers manufactured on blades and flakes (Graf & Buvit, 2017; Pitulko et al., 2017). Many of these assemblages, especially those found in central Alaska, have been assigned to the Nenana technological complex (Goebel et al., 1991; Hoffeecker et al., 1993; Powers & Hoffeecker, 1989; Younie & Gillispie, 2016).

Some colleagues have argued that all sites should be subsumed into a single Beringian Tradition in which at times ancient Beringians would select either a microblade-based toolkit or a non-microblade-based toolkit, depending on the behaviors to be performed at sites during different seasons of occupation (Holmes, 2001; Potter, 2008; Potter et al., 2013; Wygal, 2018). By grouping potentially chronologically distinct industries together without support from robust site-function and seasonality data, however, such interpretations

mask the potential significance of the variability present, especially when chronological patterning is found between technological complexes (Graf et al., 2015). Certainly, recent paleogenomic studies contend that Beringia was inhabited by at least two, and possibly more than two, ancient Beringian populations (Moreno-Mayar, Potter, et al., 2018; Moreno-Mayar, Vinner, et al., 2018). Therefore, a detailed study of the depositional, geoarchaeological contexts of multicomponent sites with both sets of industries is warranted before the field can adequately access the meaning of the variability. Only a few Beringian sites have multiple terminal Pleistocene components where assemblages ascribable to both technological complexes occur in straightforward geological contexts that can be used to assess the significance of this technological (and presumably subsistence and land-use) variability. The Owl Ridge site is one such location, as it has three terminal Pleistocene-aged components.

Another interesting research context of late Pleistocene archaeology in Beringia, especially in interior Alaska, is the climatic and environmental context in which this record formed. The sites located in the Nenana Valley, near Owl Ridge, are situated on high, ancient alluvial terraces of the Nenana River and its tributaries. During the late Pleistocene, when people were first visiting these locations, glaciers were far upstream in the mountains of the Alaska Range, and the landscape was treeless with a vegetation community transitioning from herb-tundra to shrub-tundra (Graf & Bigelow, 2011). The faunal community was transitioning from extinct (e.g., mammoth and horse) to relatively extant species (e.g., bison, wapiti, and sheep), though bison were present in small numbers in the herb-tundra biome and wapiti went extinct as shrub-tundra gave way to boreal forest (Guthrie, 2006; Hoffeecker, 1988; Powers et al., 2017). High terraces at the locations of the Dry Creek, Moose Creek, Walker Road, Panguingue Creek, Little Panguingue Creek, and Owl Ridge as well as the exposed bedrock ridge at Teklanika West provided hunters with good lookouts for faunal resources.

The archaeological materials at these sites are positioned in unconsolidated, fine sediments (silts and sands), and previous work in the region has established their mostly eolian depositional nature (Begét, Bigelow & Powers, 1991; Bigelow, Begét, & Powers, 1990; DiPietro, Driese, Nelson, & Harvill, 2017; Hoffeecker, 1988; Thorson & Hamilton, 1977; Waythomas & Kaufman, 1991). Regarding site formation and climatic interpretation based mostly on sediment data, there has been some debate as to whether a certain eolian depositional unit called “Sand 1,” first identified at the Dry Creek site and subsequently documented at other sites (e.g., Walker Road, Owl Ridge, Little Panguingue Creek) represents a regional chronostratigraphic marker signaling the Younger Dryas interval (Begét et al., 1991; Bigelow et al., 1990; Gómez Coutouly, Graf, Gore, & Goebel, 2019; Hoffeecker, 1988; Thorson & Hamilton, 1977), or a series of independent, local events when proximately available sediment blew onto these locations (Waythomas & Kaufman, 1991). Another contested point relates to whether all eolian deposits in the area resulted from the same sediment source (Bigelow et al., 1990), or if coarser sand deposits originated from a southern katabatic-wind source in the Alaska Range while finer loess deposits originated from

a more northeastern, Nenana River or Tanana River streambed source (DiPietro et al., 2017; Muhs & Budahn, 2006). All are important concerns when interpreting regional climate and environment at these sites and considering human response to changing conditions.

From 2007 to 2010, our team conducted full-scale excavations at the remote location of Owl Ridge. As discussed below, site testing in the 1970s and 1980s established three cultural components present at the site, a Nenana complex component, a Denali complex component, and a much younger component; however, early attempts at radiocarbon dating these were problematic and no clearly diagnostic artifacts were found. Therefore, we revisited the site with a set of specific research goals. First, we wanted to excavate enough of the site to provide a representative artifact assemblage of each component. Second, we wanted to search for cultural features that would preserve datable materials for effectively establishing site chronology. Third, we wanted to assess site stratigraphy and geological integrity of the components. If we met these immediate goals, then our long-range objectives were to assess whether a Nenana complex occupation exists at Owl Ridge that is separate stratigraphically, chronologically, and technologically from a Denali complex occupation, to replicate the pattern at Dry Creek, and to further examine diachronic change in technological and hunting strategies in relation to changing climate, thereby informing on the regional settling-in process by ancient Beringians. With this paper we present our observations of site stratigraphy, radiocarbon chronology, sedimentology, and basic lithic variability to assess geological integrity and natural site formation. Details regarding technological variability represented by component lithic assemblages are presented elsewhere (Gore & Graf, 2018). We use Owl Ridge as a case study to test the hypothesis that in the greater Nenana Valley region of eastern Beringia there are reliable paleoenvironmental and archaeological chronostratigraphic marker horizons reflecting depositional environments associated with regional terminal Pleistocene-Holocene climatic events, and that well-dated archaeological complexes sequentially represent initial human dispersal into the valley, settling-in, and continued response to climate change.

2 | MATERIALS—OWL RIDGE BASICS

The Owl Ridge site (FAI-091) is located along the northernmost flank of the northern foothills of the Alaska Range, about 125 km southwest of Fairbanks, Alaska, and is positioned on a south-facing glacial outwash terrace along the east side of the Teklanika River, approximately 80 m above the confluence of First Creek with the river (Figure 1). As mentioned above, this geomorphological setting is not unique in the region, where terminal Pleistocene sites often sit atop ancient alluvial terraces incised by side-valley streams, affording occupants long views of the surrounding territory (Powers & Hoffecker, 1989).

Owl Ridge was first discovered in 1976 by D. C. Plaskett and R. M. Thorson during a backpacking reconnaissance trip (Plaskett,

1976). At that time, they excavated three test pits to assess the site's potential for buried cultural materials. They found two possible cultural components in one test pit and nothing in the other two test pits. Thorson and Hamilton (1977) reported a cobble feature from the lower of the two components. Under the direction of W. R. Powers, a small University of Alaska Fairbanks (UAF) field crew revisited the site in 1977–1978, excavating several additional small test pits. They also re-exposed the cobble feature, determined its cultural origin, and collected a peat sample from a paleosol directly underlying the feature's stones, obtaining an age of $9,325 \pm 305$ (GX-6283) ^{14}C years BP. They also documented the eolian stratigraphy of the site's deposits (Hoffecker, 1988; Hoffecker et al., 1996; Phippen, 1988).

In 1982 and 1984 P. G. Phippen and three field assistants returned to the site to continue the testing project. In total, they opened about 26 m² and documented three cultural components within eight stratigraphic units. Components consisted of small lithic assemblages, totaling less than 1,000 pieces. The unconsolidated silt and sand deposits of the site were described as averaging about 125 cm in total thickness. According to Phippen (1988), Component 1 was found in lithostratigraphic unit (Stratum) 2, lowermost silt overlying basal glacial outwash (Stratum 1). Mantling Stratum 2 was a medium-coarse sand lens, Stratum 3. Stratum 4, silty sand containing a well-developed paleosol complex, contained Component 2. Artifacts were found associated with the paleosol. Overlying Stratum 4 was a package of bedded sands (Stratum 5), and Component 3 was reported from the contact zone between Stratum 5 and the overlying silty sand-labeled Stratum 6. Phippen (1988) interpreted Strata 2, 4, and 6 as loess deposits and Strata 3 and 5 as eolian bluff-edge (or cliffhead) sand deposits. To explain the bedding of Stratum 5, Phippen (1988, p. 101) proposed that an overland erosional event following deposition of Stratum 4 eroded material from Strata 4 to 3, redepositing it just over the terrace edge directly below the site and providing an immediate sediment source for Stratum 5 to be blown onto the site as cliffhead sands. He argued recurrent periods of strong winds deflated the middle section of Stratum 5, leaving behind lags (gravel lenses) in that section and creating the bedding observed. Phippen (1988) obtained 12 radiocarbon dates for the stratigraphic sequence he described (Table 1). He found no clearly diagnostic artifacts and instead used radiocarbon dates to ascribe Component 1 to the Nenana complex, dating to about 13,300 cal yr BP; Component 2 to the Denali complex, dating to about 11,000–8,000 cal yr BP; and Component 3 to a nonspecific archaeological complex postdating 8,000 cal yr BP (Hoffecker et al. 1996; Phippen, 1988).

That the site had only been systematically tested (~33 m²) with dispersed 1-m² test units, with very little of Component 1 being excavated (~6–7 m²), we pursued large-scale block excavations to address our goals stated above. Below we review the methods we used both in the field and in the lab, present field, and lab results, and discuss these results in the context of project research goals.

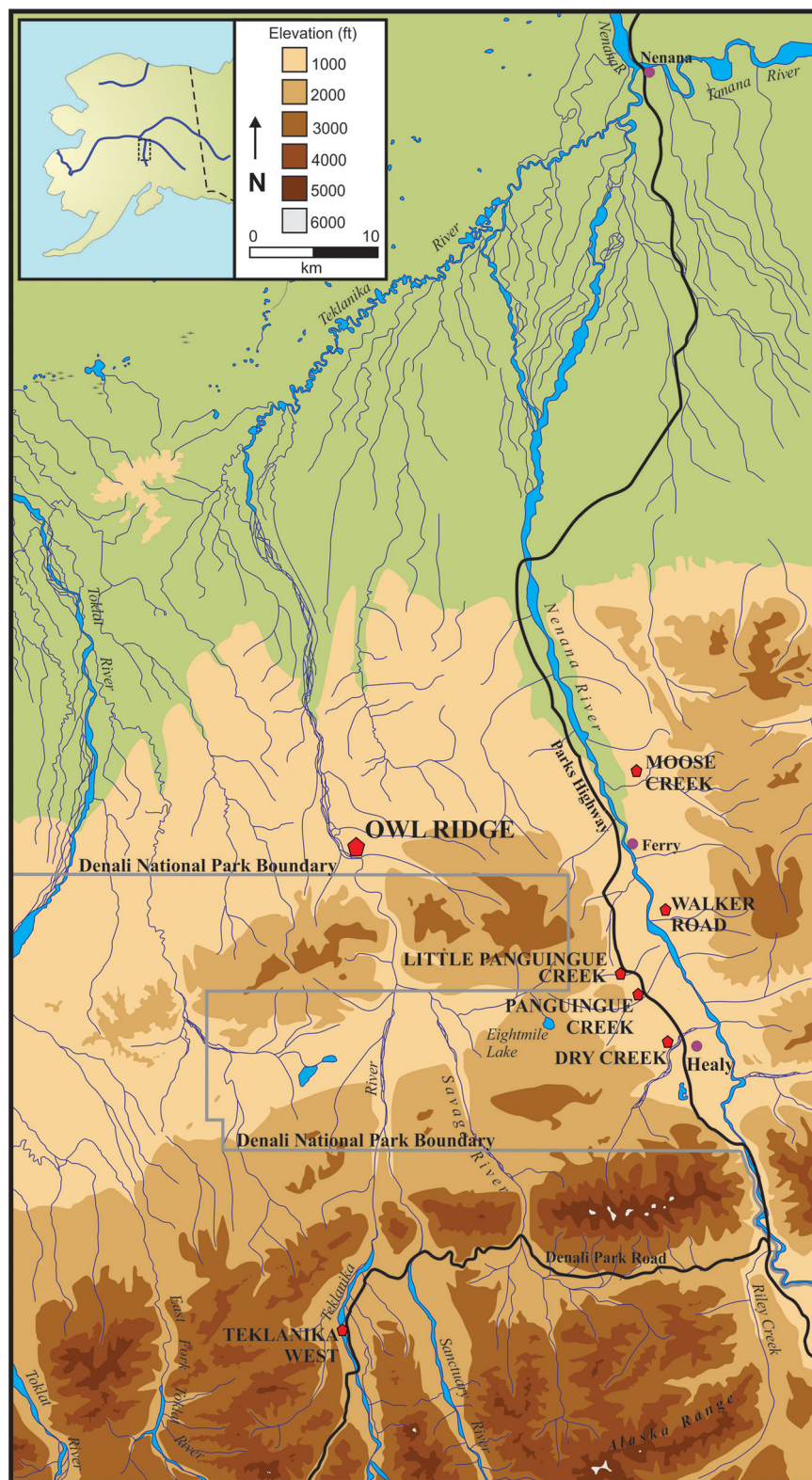


FIGURE 1 Location map of Owl Ridge. Note locations of other sites mentioned in the text [Color figure can be viewed at wileyonlinelibrary.com]

TABLE 1 Radiocarbon dates from excavations of the Owl Ridge archaeological site

Stratum	Component	Square	Material	Lab number	¹⁴ C age BP (1σ)
Conventional radiocarbon dates from previous investigations ^a					
6 (upper)	–	N88E105	Charcoal	D-3071	930 ± 50
6 (middle)	–	N90E111	Charcoal	Beta-11080	4,400 ± 70
5/6 contact	3	N88E105	Charcoal	Beta-11082	1,480 ± 110
5/6 contact	3	N91E108.5	Charcoal	D-3070	6,900 ± 265
5 (upper)	3	N91E111	Charcoal	GX-13009	7,035 ± 380
4	2	N88E105	Charcoal?	Beta-11081	2,470 ± 120
4	2	N90E95	Organic/soil	Beta-11437	7,230 ± 100
4	2	N93.5E100	Organic/soil	Beta-11436	7,660 ± 100
4	2	N93.5E100	Organic/soil	Beta-5418	8,130 ± 140
4	2	N94.5E99.5	Peat/organic	GX-6283	9,325 ± 305
2	1	N90.5E101	Charcoal?	Beta-11079	2,380 ± 90
2	1	N86.5E105	Charcoal	Beta-5416	9,060 ± 410
2	1	N90E111	Charcoal	Beta-11209	11,340 ± 150
AMS radiocarbon dates from current study ^b					
6 (middle)	–	N92E110	Charcoal (<i>Picea</i> sp.)	Beta-289381	4,450 ± 40
6 (base)	–	N92E110	Charcoal (<i>Picea</i> sp.)	Beta-289380	4,380 ± 40
5 ^c	3	N92E110	Charcoal (<i>Salix</i> sp.)	Beta-289379	9,790 ± 40
5 ^c	3	N92E110	Charcoal (<i>Salix</i> sp.)	Beta-330172	9,880 ± 40
6/5/4 ^d	3/2	N83E105	Charcoal (<i>Salix</i> sp.)	Beta-289376	9,550 ± 40
6/5/4 ^d	3/2	N83E105	Charcoal (<i>Salix</i> sp.)	Beta-289377	10,080 ± 40
4	2	N95E98	Charcoal (<i>Picea</i> sp.)	Beta-289382	80 ± 40
4	2	N86E108	Charcoal (<i>Salix</i> sp.)	Beta-289378	10,020 ± 40
4	2	N88E105	Charcoal (<i>Salix</i> sp.)	AA-86967 ^e	10,120 ± 75
4	2	N88E105	Charcoal (<i>Salix</i> sp.)	UCIAMS-71260 ^e	10,125 ± 20
4	2	N86E106	Charcoal (<i>Salix</i> sp.)	AA-86966	10,290 ± 75
4	2	N86E104	Charcoal (<i>Salix</i> sp.)	AA-86965	10,295 ± 60
4	2	N86E103	Charcoal (<i>Salix</i> sp.)	AA-86961	10,330 ± 70
4	2	N86E103	Charcoal (<i>Salix</i> sp.)	AA-86963	10,340 ± 75
4	2	N86E103	Charcoal (<i>Salix</i> sp.)	AA-86962	10,355 ± 60
4	2	N86E103	Charcoal (<i>Salix</i> sp.)	AA-86960	10,415 ± 60
4	2	N86E104	Charcoal (<i>Salix</i> sp.)	AA-86964	10,420 ± 60
4	2	N85E103	Charcoal (<i>Salix</i> sp.)	AA-86968 ^e	10,440 ± 60
4	2	N85E103	Charcoal (<i>Salix</i> sp.)	UCIAMS-71261 ^e	10,485 ± 25
2	1	N88E110	Charcoal (<i>Salix</i> sp.)	AA-86969	11,060 ± 60

^aPreviously reported dates are uncorrected (Hoffecker et al., 1996; Phippen, 1988).

^bAMS dates reported here are corrected for isotopic fractionation following Stuiver and Polach (1977).

^cSample from hearth feature F10.01. Only two samples directly dating a cultural feature.

^dSamples obtained from a compressed area at the edge of the terrace where Strata 6, 5, and 4 could not be confidently separated during excavation.

^eThese are sample splits submitted to both Arizona AMS lab and Tom Stafford/UCIAMS, respectively.

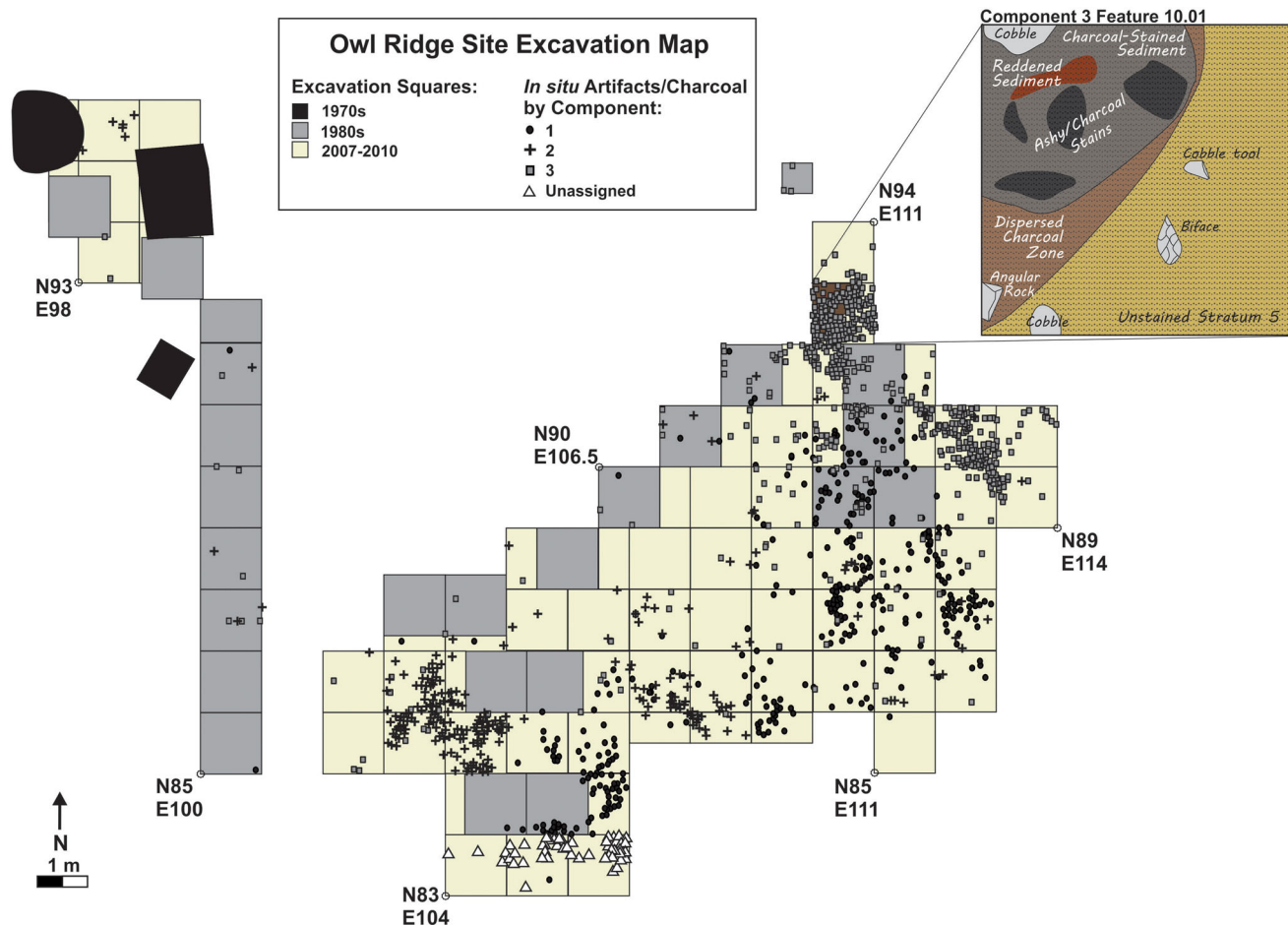


FIGURE 2 Excavation map showing the 2007–2010 excavation squares relative to those from previous investigations as well as the distribution of all artifacts by component found at the site and a blow-up map of hearth feature F10.01 associated with Component 3 [Color figure can be viewed at wileyonlinelibrary.com]

3 | EXCAVATION METHODS AND POST-FIELDWORK ANALYTICAL PROCEDURES

3.1 | Excavation methods

During our 2007, 2009, and 2010 excavations we significantly extended previously excavated test squares from the 1970s and 1980s projects to assess geological and archaeological integrity of the site as well as to better understand changing activity areas and behavioral adaptations represented (Figure 2). A total of 58 m² were excavated in two blocks and six geological test units (GTUs). A small block was excavated by opening approximately 4 m² that connected four dispersed test units (roughly 4.75 m²) previously excavated in the 1970s/1980s, making an 8.5-m² block where the reported cobble feature was observed (Phippen, 1988; Plaskett, 1976). Our larger block consisted of about 48 m² that connected 14 dispersed 1-m² test squares previously excavated by Phippen (1988), ultimately forming an approximately 62-m² block. We followed standard archaeological excavation procedures and maintained the original grid established in the 1980s with an arbitrary N100E100Z100 datum point placed near the

apex of the terrace ridge so that all excavation squares placed on the Owl Ridge terrace would maintain positive northing, easting, and elevation coordinates, and would roughly correspond to previous work.

Prior investigations found no cultural materials in the upper 30–40 cm of the profile (Phippen, 1988); therefore, we removed the surface root mat associated with the modern soil with flat shovels, excavating and screening the root mat in 5-cm-thick levels. Below the root mat, we removed the remaining sediment by hand troweling. Following removal of the root mat, every 1 m² was subdivided into four 50-cm² quadrants to maintain horizontal control and excavated in 5-cm-thick levels within recognizable natural stratigraphic units to maintain vertical control of site sediments. All sediment from site deposits was dry screened through 1/8-in. mesh. Artifacts and charcoal recovered in situ were recorded with three-point provenience using a Sokkia EDM total station. Trend and plunge (i.e., dip direction and angle) of artifacts were measured using Silva Ranger clinometer compasses when the artifact's original aspect could be confidently assessed. Materials recovered from screening were assigned to their respective quadrant, 5-cm level, and geological stratum. The top of each new stratum was exposed, mapped, and

photographed before its excavation commenced. All postdepositional disturbances were documented in plan views for each stratigraphic boundary and recorded in site profiles when possible. Sediment and stratigraphy were described, and profiles were photographed and drawn in the field. From an exposed excavation wall in the main block, we collected two sets of sediment samples, a set of discrete, “grab” samples from each stratum and a set of samples from a continuous sediment column. Micromorphological samples were collected by driving plastic conduit boxes, measuring 3.75” long by 2.25” wide by 2.90” deep, into exposed excavation faces and profile walls. Samples encased in the boxes were removed with provenience and orientation information recorded in the field. Below we present preliminary particle size distribution results from the discrete stratum samples. More detailed particle size and bulk chemistry data from the continuous column as well as the micromorphological results are presented elsewhere (DiPietro, Graf, Driese, & Stinchcomb, in review).

To further assess the depositional context and processes forming the various stratigraphic units of the site, we also excavated six 1-m² GTUs along the apex of the ridge on which the site rests. Beginning on site, GTU-1 was placed at grid point N107E99 at the far northern margin of the site at the apex of the ridge. GTU-2 was placed approximately 150 m upslope and northeast of GTU-1. The next three GTUs (3–5) were placed every 100 m farther upslope. Finally, GTU-6 was placed approximately 900 m upslope (Figure 3). We used a handheld Garmin GPS unit to determine their locations relative to

the site. We excavated each GTU with flat shovels in 50-cm² quadrants and 10-cm arbitrary levels within natural geological strata, and we screened all sediment through 1/8” mesh in the event that archaeological materials or ecofacts occurred. We recorded the stratigraphic profile of each geological test square.

3.2 | Postfieldwork analytical procedures

Charcoal samples for radiocarbon analysis were identified taxonomically using plant reference collections and libraries at the Desert Research Institute (Reno) and Department of Anthropology at Texas A&M University. All samples were collected from three-point-provenience contexts in the excavation, except for one which was collected from a hearth fill sample. Most samples were prepared, pretreated, and analyzed at the National Science Foundation–Arizona Accelerator Mass Spectrometry Facility (AA) and Beta Analytic, Inc. (Beta). Two samples were prepared and pretreated by Tom Stafford and analyzed at the W. M. Keck Carbon Cycle Accelerator Mass Spectrometry facility at the University of California, Irvine (UCIAMS). Physical preparation and chemical pretreatment of samples followed regular procedures (Jull, Donahue, & Zabel, 1983). All ¹⁴C ages were $\delta^{13}\text{C}$ -corrected for isotopic fractionation following Stuiver and Polach (1977) and calibrated and modeled with OxCal 4.3.2 (Bronk Ramsey, 2017) using the IntCal13 northern hemisphere atmospheric curve (Reimer et al., 2013). Before calibration and modeling, we used the “combine” function in Oxcal to obtain

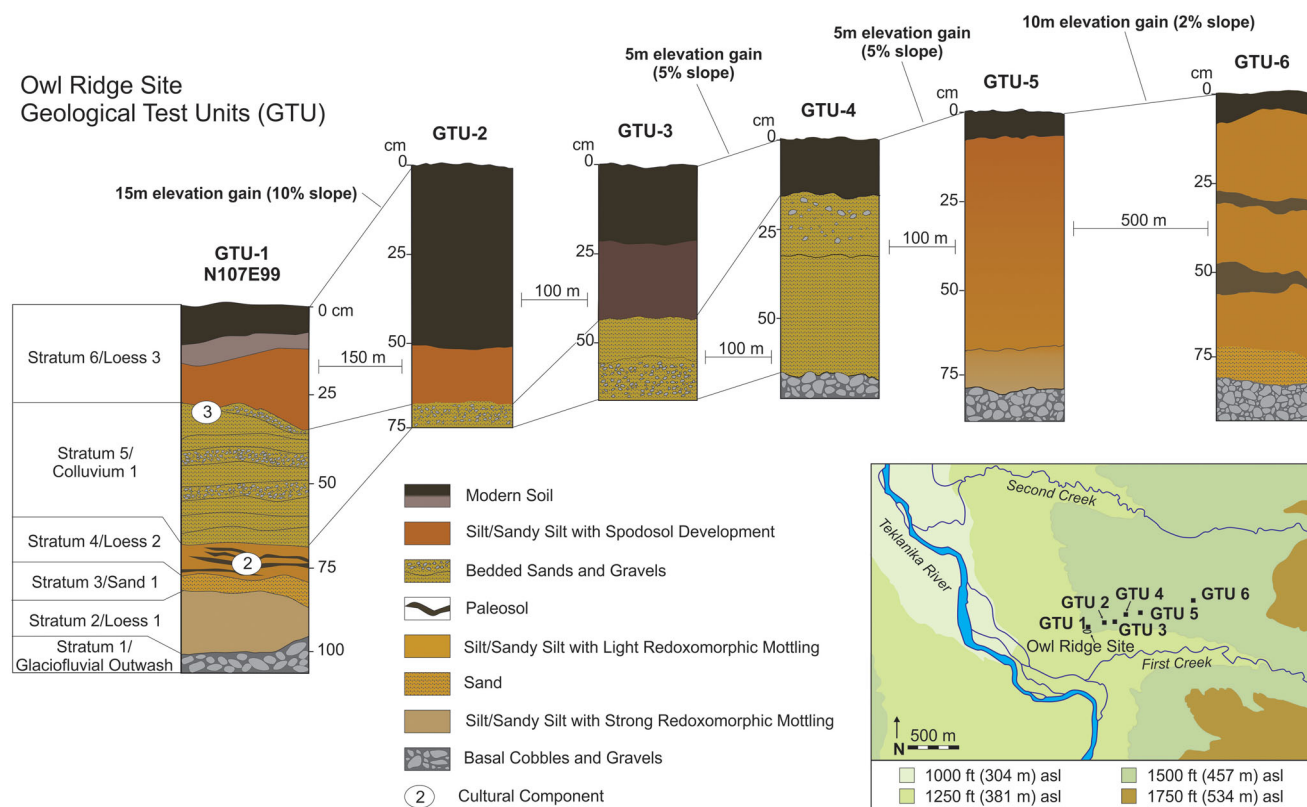


FIGURE 3 Stratigraphic correlations of geological test units and a location map showing the position of the GTUs relative to the site. GTU, geological test unit [Color figure can be viewed at wileyonlinelibrary.com]

weighted means on two separate sets of split samples as well as paired dates obtained on a hearth feature, following the methods outlined in Ward and Wilson (1978) after testing for contemporaneity (χ^2 test).

Particle-size distributions presented here were obtained at the Texas A&M University Soils Characterization Laboratory. Samples were dry sieved through a 2-mm sieve. Particle-size distributions of fines were obtained by wet sieving, settlement, and the pipette method (outlined in Kilmer & Alexander, 1949) after pretreating each 10-g sample by dispersion with sodium hexametaphosphate. The percentage of coarse fraction was calculated, and measured fractions include very fine gravels (4–2 mm) and material greater than 4 mm. Measured fine fractions include very coarse sand (2–1 mm), coarse sand (1 mm–500 μ m), medium sand (500–250 μ m), fine sand (250–100 μ m), very fine sand (100–50 μ m), coarse-medium silt (50–5 μ m), fine silt (5–2 μ m), coarse-medium clay (2 μ m–200 nm), and fine clay (<200 nm).

Lithic artifacts were cataloged and analyzed for typological, technological, and site formation studies at Texas A&M University. Artifacts were visually inspected using a $\times 10$ -hand lens and analyzed following an analytical protocol for early period archaeological assemblages of Alaska and Siberia developed by the lead author (Graf, 2008, 2010; Graf & Goebel, 2009). Basic descriptive variables and lithic technological organization variables specific to raw-material procurement and selection behaviors have been presented elsewhere (Gore & Graf, 2018). Below we briefly present the lithic assemblage, with analyses focusing on two sets of variables to assess geoarchaeological site formation: artifact plunge and trend and

artifact refits. These variables permit assessment of the degree of postdepositional movement of archaeological materials at the site.

4 | RESULTS

4.1 | Field observations at Owl Ridge

4.1.1 | Site stratigraphy

During our excavations, we identified three cultural components and found them resting within a package of unconsolidated fine sediments with an overall thickness of about 125 cm, slope aspect of approximately 185° southwest of true north, and 12% or 7° slope gradient. This package of sediment was positioned unconformably atop ancient glacial outwash of matrix-supported gravels and cobbles presumed to correspond to the Healy glaciation erosional terrace (Ritter, 1982; Thorson, 1986) of early MIS-3 age ($\geq 55,000$ years ago) (Dortch, Owen, Caffee, Li, & Lowell, 2010). We observed the same basic stratigraphic sequence previously described (Hoffecker et al., 1996; Phippen, 1988) and generally maintained original stratigraphic designations; however, we found Phippen's (1988) Strata 8 and 7 to be genetically tied to underlying Stratum 6. The entire stratigraphic profile is characterized below (Figure 4).

Stratum 1 forms the base of the profile and consists of weathered beds of poorly sorted fine, medium, and coarse sands with larger subrounded stone clasts grading in size from gravels to small boulders (several clasts 2–10 cm in diameter). As mentioned above,

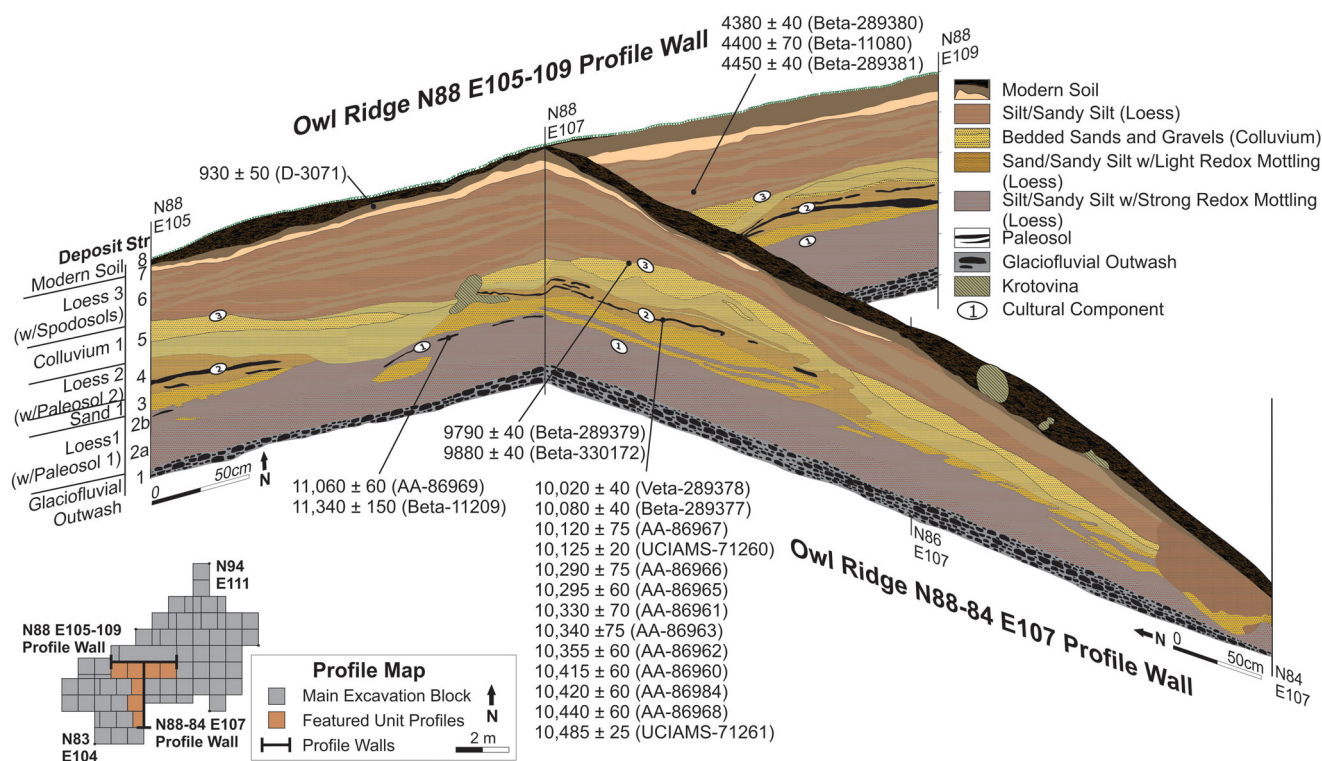


FIGURE 4 Representative stratigraphic profiles of the site [Color figure can be viewed at wileyonlinelibrary.com]

this stratum represents an ancient alluvial remnant of a glacial outwash terrace of the Teklanika River.

Stratum 2 forms an abrupt (0.5–2 cm zone) boundary with underlying Stratum 1, measuring 20–30 cm in total thickness. We subdivided it in the field based on observed textural and color differences. The lower section, 2a, is composed of a relatively compact dark grayish brown (2.5Y 4/2) silt with tight cohesiveness, measures about 10–15 cm in thickness, is frozen when encountered, and has massive structure. Stratum 2a requires several days to thaw before being excavated. It contains few coarse sand grains near its base, likely inherited from underlying Stratum 1. Stratum 2b is composed of a cohesive, pale yellow (2.5Y 7/4) to olive brown (2.5Y 4/3) sandy silt with brownish yellow (10YR 6/6) redoximorphic (redox) masses. It measures about 10–15 cm in thickness and has a weak platy structure. Redox masses resulted from periods of alternating reduction and oxidation of iron compounds, and platy structure resulted from ice-lens formation. A very faint buried A horizon (strong brown; 7.5YR 5/6), Paleosol 1, was observed in the upper 5–10 cm of Stratum 2b during excavation; however, it was not observed in the field as a soil feature that could be consistently mapped. We found a discrete layer of lithic artifacts, Component 1, and a few pieces of dispersed charcoal, associated with Paleosol 1 in Stratum 2b. Stratum 2 appears to be relatively uniform in thickness and appearance across the site; it maintained a 20–30-cm thickness both near the terrace edge and at the apex of the ridge.

Stratum 3 consists of poorly sorted, mostly coarse sand and medium sand. It ranges from dark olive brown (2.5Y 3/3) to olive brown (2.5Y 4/3) in color. This stratum averages about 10 cm in thickness and generally increases in thickness toward the terrace edge. With underlying Stratum 2b, it forms an abrupt boundary that ranges from smooth in some places to convoluted in others, expressing some minor downslope creep with solifluction folds measuring 1–5 cm vertical distance over 5–15 cm horizontal distance.

Stratum 4 forms a distinct (2–5 cm zone) boundary with underlying Stratum 3 and is composed of a cohesive, very dark grayish brown (10YR 3/2) to dark grayish brown (10YR 4/2) silty sand near its base, grading to sandy silt toward its top, with strong brown (7.5YR 5/6), horizontally-oriented linear-shaped redox masses throughout. Generally, this stratum ranges from 10 to 20 cm in thickness, mostly maintaining its thickness across the site surface except for immediately at the terrace edge where it abruptly thins. Its lower 5 cm contains more medium-to-fine sand grains likely inherited from underlying Stratum 3. The sand portion of the Stratum 4 matrix becomes finer from bottom to top, and a strong, very dark brown (10YR 2/2) buried A horizon, Paleosol 2, is present within the stratum. Redox masses in Stratum 4 indicate postdepositional periods of alternating wet-dry conditions, and the stratum shows clear signs of downslope creep with solifluction folds of 3–10 cm vertical distance over 10–15 cm horizontal distance. The top of Stratum 4 forms an abrupt, smooth boundary with overlying Stratum 5. Component 2 artifacts were observed in a 5–10 cm thick zone just above, within, and below Paleosol 2. Because the stratum

experienced a period of relatively significant cryoturbation, some artifacts may have been displaced from an original paleosol association; however, none appear to have moved outside of Stratum 4.

Stratum 5 is characterized by light olive brown (2.5Y 5/4) to pale yellow (2.5Y 7/4) bedded sands and gravels, forming an abrupt, smooth boundary with underlying Stratum 4. Across most of the excavated portion of the site, we observed a general pattern of three discernable beds 5–15 cm in thickness in Stratum 5, though as many as nine beds were observed at the north end of the site near the apex of the ridge opposite the terrace edge. The stratum, therefore, is thickest upslope (45–40 cm thick) and thins toward the terrace edge (10–5 cm thick). Typically the uppermost and lowermost beds are characterized by structureless, medium sand with some finer and coarser sands mixed within. The middle bed is typically coarser in texture, often with lenses of subrounded-to-rounded, fine-to-coarse gravels. Upslope where several beds are present, they alternate between coarser and finer sediment, grading from coarse sands with gravels to finer sands with silt. Within beds the sediment is poorly-to-moderately sorted. The boundary with overlying Stratum 6 is gradual (5–10 cm thick). Component 3 is mostly found in the upper 5 cm of Stratum 5, but 27% of Component 3 artifacts were observed in the boundary zone of these layers, and 19% were found in lowermost Stratum 6.

Stratum 6 is described as variable in color with alternating zones of dark brown (7.5YR 3/2), pinkish gray (7.5YR 6/2), reddish brown (7.5YR 6/6), very dark grayish brown (10YR 3/2), and dark brown (10YR 3/3), variations which appear to result from soil imprinting on unweathered dark yellowish brown (10YR 4/4) sandy silt-to-silty sand. Discrete paleosol horizons were not traceable across the site. The stratum varies in thickness from about 40–70 cm in which it is thickest in the center of the site excavation and thins both toward the apex of the ridge and at the terrace edge. Stratum 6 generally has a granular structure; however, weak platy bodies were also observed. Root zones associated with charcoal from burning forest material were present, especially in the upper 10 cm of the stratum, but several root-burn features were present throughout the stratum. In agreement with previous reports (Hoffecker et al., 1996; Phippen, 1988), we found some artifacts in the lowermost 2–5 cm of Stratum 6 associated with its contact with Stratum 5. We tentatively assigned these artifacts to Component 3, and for reasons discussed below, we maintain that assignment.

Stratum 7 is a light gray (10YR 7/2) to grayish brown (10YR 5/2) sandy silt generally 5–15 cm thick. This stratum contained discontinuous root/organic zones of both charred and uncharred material. Its lower contact with Stratum 6 is gradual and wavy.

Stratum 8 forms an abrupt, smooth boundary with Stratum 7, measures about 5–15 cm in thickness, and consists mostly of the modern root mat and decaying organic materials associated with the current forest floor.

Strata 6–8 were originally defined as separate stratigraphic units by Phippen (1988), but we interpret these to be genetic soil horizons of the modern soil solum, with Stratum 8 the O horizon, Stratum 7

the E horizon, and Stratum 6 the well-developed B horizon and C horizon of the modern soil. The coloration patterns observed in the upper 2/3 of Stratum 6 indicate postdepositional illuviation of organic matter and sesquioxides originating in the overlying O/E horizons.

4.1.2 | Geological test units

Figure 3 illustrates map locations and profiles from six GTUs excavated along the apex of the ridge, beginning near the northern edge of the site (GTU-1) and running upslope to nearly 1 km northeast of the site (GTU-6). We excavated each from the surface to basal cobbles and gravels, except for GTU-2 and GTU-3 where we encountered frozen sediment at nearly 75 cm below the surface. Both of these test units were located in areas of heavy vegetation cover, and despite leaving both open for 5 weeks, they never thawed. We found three artifacts in GTU-1 (located at N107E99 on our site grid), including one flake fragment from Stratum 4 (Component 2) and one flake fragment and one flake from the Strata 5/6 contact (Component 3). All other GTUs were negative for archaeological materials. Below we highlight patterns that inform on-site formation at Owl Ridge.

We recognized that Stratum 5, bedded sands, and gravels, generally increased in thickness upslope from the site. Though we were unable to completely excavate this stratum in GTU-2 and GTU-3 due to perennially frozen ground, it was present near the base of these squares (basal ~5 cm in GTU-2 and basal 25 cm in GTU-3). Its thickness was only 35–40 cm in GTU-1 nearest the site, and within the main excavation block it ranged in thickness from about 5 to 25 cm, thickening upslope away from the terrace edge, and was found to be 50–55 cm thick in GTU-4. GTU-5 and GTU-6, situated about 0.5 and 1 km upslope from the site and on higher (about 25 m and 35 m, respectively) surfaces, do not have Stratum 5 in their profiles. We contend that Stratum 5 originated through the overland flow of sediments from upslope of the site, likely from the higher terrace risers upon which GTU-5 and GTU-6 are located.

Another interesting pattern with regard to Stratum 5 is that, unlike in the main excavation, GTU-1 expresses nine beds of sands and gravels providing us with a better sense of the bedding structure within the stratum. Overall there is a general trend of sediment coarsening upward in the stratum. The uppermost beds contain bands of gravels while the lower beds are predominantly sands. From top to bottom the nine beds express four repeated shorter episodes of coarsening upward sequences. The uppermost sequence is mostly gravel overlying mostly coarse sand, overlying mostly fine sand. The next sequence is gravel and coarse sand overlying a layer of mostly fine sand. The third sequence repeats the previous one. The final sequence is coarse sand overlying fine sand. Though we have recognizable bedding, sediment within each bed is poorly sorted. Overall the bedding pattern of Stratum 5 signals overland flow deposits. Certainly, the thickening of this stratum upslope of the site and terrace edge supports the interpretation that Stratum 5 is

colluvial in origin, and not eolian as initially interpreted by Phippen (1988).

4.2 | Radiocarbon chronology

4.2.1 | New radiocarbon dates

From our renewed excavations we obtained 20 new AMS radiocarbon dates for the deposits at Owl Ridge (Table 1). One of our original excavation objectives was to find cultural features preserving wood charcoal for directly dating the site's cultural occupations. We found only one hearth feature, F10.01, to accomplish this goal. It was isolated in the uppermost bed of Stratum 5 in N92E110 and was surrounded by a lithic-reduction artifact cluster of Component 3 (Figure 2). Two of the 20 new dates were obtained on samples from this feature, but the remaining dates were obtained from identified wood charcoal fragments from stratigraphic contexts, not clearly from cultural features. Below we review these new dates as well as previously reported dates to develop a reliable chronostratigraphic sequence for the site.

Despite our best efforts, only three charcoal samples were observed and collected from a Stratum 2 stratigraphic context, and of these, only one was large enough to be confidently taxonomically identified before being submitted for AMS dating. The result is a new age estimate of $11,060 \pm 60$ (AA-86969) ^{14}C BP on willow (*Salix* sp.) wood charcoal from Paleosol 1, Stratum 2b, associated with a Component 1 artifact cluster. No charcoal samples were preserved in Stratum 3.

Thirteen samples from various artifact clusters associated with Paleosol 2, Stratum 4, were dated. Twelve of these ranged in age from $10,485 \pm 25$ (UCIAMS-71261) to $10,020 \pm 40$ (Beta-289378) ^{14}C BP and were obtained on wood charcoal identified as willow (*Salix* sp.). A single sample identified as spruce (*Picea* sp.), which seemed out of place because white spruce (*P. glauca*) is thought to have invaded the area several millennia later (Edwards et al. 2001), not surprisingly returned a modern age estimate of 80 ± 40 (Beta-289382) ^{14}C BP. We maintain this sample and date resulted from recent intrusion of spruce-tree roots into Stratum 4 and then subsequent burning.

Two dates of 9880 ± 40 (Beta-330172) and 9790 ± 40 (Beta-289379) ^{14}C BP were obtained on wood charcoal (*Salix* sp.) from the F10.01 hearth feature in upper Stratum 5, directly dating cultural activity of Component 3 in this area of the site.

Strata 4–6 were compressed in an area adjacent to the terrace edge (N83E104–106), so clear separation of these strata and associated materials could not be obtained in the field. In an attempt to remedy this situation, we submitted two wood charcoal (*Salix* sp.) samples found adjacent to artifacts in this context from the same square and within 5 cm elevation of each other. The lower sample yielded a date of $10,080 \pm 40$ (Beta-289377) ^{14}C BP, and the upper sample produced a younger date of 9550 ± 40 (Beta-289376) ^{14}C BP. These dates do not overlap each other at 2σ standard deviation. The older date, however, overlaps with seven of the Stratum 4 dates presented above, but the younger date does not overlap with our

Stratum 5 dates. In fact, the Stratum 5 dates predate it by at least 80 ^{14}C years.

Finally, two dates of $4,380 \pm 40$ (Beta-289380) and $4,450 \pm 40$ (Beta-289381) ^{14}C BP were obtained on charcoal identified as *Picea* sp. The former date's sample came from the base of Stratum 6, while the latter sample came from a rather large concentration of charcoal that appeared to be a charred log or large spruce root about 15 cm higher in the profile in the middle of Stratum 6. Because both samples were spruce, came from the same square, and provide statistically similar ages, we assume that they represent the same burn event and may be from the same spruce-tree root complex. They provide an age of the middle of Stratum 6.

4.2.2 | Comparison with previous conventional dates

Comparing the entire list of 33 radiocarbon dates, we see quite a bit of incongruity, especially between new AMS dates and conventional dates obtained in the 1970s and 1980s (Table 1). Conventional dates were mostly obtained on unidentified materials or questionable substances such as soil organics. A few were very small in size so the conventional technique resulted in ages with very large standard errors making them useless for dating depositional events. Of the 13 previously obtained dates, 10 are very clearly discordant. These problematic dates are discussed below, before presenting an age model for the site.

There are now four dates from Stratum 2, one reported here of $11,060 \pm 60$ (AA-86969) ^{14}C BP and three previously reported dates of $11,340 \pm 150$ (Beta 11209), $9,060 \pm 410$ (Beta-5416), and $2,380 \pm 90$ (Beta-11079) ^{14}C BP (Table 1). The two dates of $11,340 \pm 150$ (Beta 11209) and $11,060 \pm 60$ (AA-86969) ^{14}C BP provide concordant ages that overlap at 2σ . The dates $9,060 \pm 410$ (Beta-5416) and $2,380 \pm 90$ (Beta-11079) ^{14}C BP, however, are discordant and even postdate the majority of dates from overlying Stratum 4. Further, the older one of the two has a huge standard deviation (± 410), making it useless in building a high-resolution chronostratigraphic sequence. Not surprisingly, both dates were discounted by Phippen (1988) as being the result of root intrusion from above. We concur with this interpretation.

Five previously reported dates from Stratum 4 were obtained on samples of unknown or questionable material. These include $9,325 \pm 305$ (GX-6283) ^{14}C BP on peat or unidentified organic matter; $8,130 \pm 140$ (Beta-5418), $7,660 \pm 100$ (Beta-11436), and $7,230 \pm 100$ (Beta-11437) ^{14}C BP on soil organics; and $2,470 \pm 120$ (Beta-11081) ^{14}C BP on unidentified charcoal. The youngest of these was rejected by Phippen (1988) because he surmised the sample was likely burnt spruce root. The earlier four are suspected by us to be too young because they were obtained on soil organics and were found to be in disagreement with 12 new concordant AMS dates presented above and obtained on samples with known material and provenience in Paleosol 2, Stratum 4 (see Table 1).

Phippen (1988) reported two wood charcoal samples from the Stratum 5/6 contact. One sample produced a date of $7,035 \pm 380$ (GX-13009) ^{14}C BP and was not identified to a taxon. The other date,

$6,900 \pm 265$ (D-3070) ^{14}C BP, was obtained on a sample of carbonized *Picea* sp. wood pieces collected from a burn feature he referred to as a possible hearth (Phippen, 1988, p. 68). He described the feature as a lens of oxidized silty sand with a concentration of charcoal running through the middle of it. There is no mention of the diameter or shape of this feature. Nor was it mapped or photographed. When excavating in the squares immediately adjacent to the test pit where Phippen reported the possible feature, we found several large *Picea* sp. charcoal pieces often mixed with uncharred, decayed-root material, mostly in the lower half of Stratum 6, from about 15 cm to within 2–5 cm of the Stratum 5/6 contact. In fact, as noted above, we dated two of these charcoal pieces (Beta-289380 and Beta-289381) and found them both to be middle Holocene in age. As presented above, we dated two pieces of short-lived *Salix* sp. wood charcoal from a mapped hearth feature (F10.01) in the upper bed of Stratum 5 to the terminal Pleistocene/early Holocene boundary. In our investigations, we found that all preserved woody samples in Stratum 6, either burnt or not, are spruce, and when dated they return Holocene ages, whereas wood charcoal samples from uppermost Stratum 5 are willow and return terminal Pleistocene ages. Based on our findings and experience excavating Stratum 6, Stratum 5, and associated Component 3 across the site, Phippen's (1988) descriptions of the feature and materials dated, as well as the nature of his early conventional dating samples, we suspect the oxidized sediment and well-preserved charcoal in his Stratum 6 feature is natural, perhaps originating from spruce root or early forest burn. Finally, the date of $1,480 \pm 110$ (Beta-11082) ^{14}C BP, also from the Stratum 5/6 contact, was obtained on wood charcoal that Phippen (1988) identified as root burn and rejected. We concur because it is more than 3,500 cal years younger than a tightly clustered series of three dates from overlying Stratum 6, obtained by both Phippen and our team.

Two new AMS dates do not fit in the emerging chronological sequence of the site. The date of 80 ± 40 (Beta-289382) ^{14}C BP also from Stratum 4 is undoubtedly aberrant for reasons stated above, and $9,550 \pm 40$ (Beta-289376) ^{14}C BP on a sample from the compressed section near the bluff edge is an outlier in the sequence and only overlaps at 2σ with two highly problematic dates from the 1980s already dismissed above (Beta-5416 and GX-6283).

Of the 33 total dates obtained from previous and current work at Owl Ridge, 12 problematic dates discussed here are outliers and do not contribute to a reliable chronology of the site. These dates not only provide discordant ages, but most were obtained on less-than-desirable sample materials or, in one case, from a compressed stratigraphic context. For these reasons, we omit them from further consideration in building the chronology for the site. Instead, we include only three conventional dates from Phippen's (1988) work found to be in concordance with our new AMS-based chronology (Table 2).

4.2.3 | Modeled, calibrated radiocarbon dates

Twenty-one radiocarbon dates, including the two sets of split dates, were accepted by us for building site chronology (Table 2). We

TABLE 2 Modeled calibration of radiocarbon dates from Owl Ridge, using OxCal v4.3.2 Bronk Ramsey (2017); r:5 IntCal13 atmospheric curve (Reimer et al., 2013)

		Prior calendar age				Posterior calendar age			
Lab number	¹⁴ C age BP (1σ)	Range	μ	2σ	m	Range	μ	2σ	m
Middle-upper Stratum 6			End middle-upper Stratum 6			93–1,472	192	877	475
D-3071	930 ± 50	930–740	844	53	846	933–742	850	52	854
Beta-289381	4,450 ± 40	5,288–4,882	5,104	112	5,102	5,286–4,882	5,098	111	5,081
Beta-11080	4,400 ± 70	5,285–4,848	5,033	127	5,007	5,283–4,847	5,028	124	5,002
Beta-289380	4,380 ± 40	5,212–4,852	4,956	76	4,942	5,211–4,851	4,954	74	4,942
			Start middle-upper Stratum 6			9,337–4,988	6,518	1,275	6,120
Component 3/Feature 10.01 (upper Stratum 5)			End Component 3/Feature 10.01 (upper Stratum 5)			11,297–7,162	10,128	1,306	10,687
Beta-289379/	9,790 ± 40	11,269–11,201	11,236 ^a	18	11,235	11,267–11,201	11,235	17	11,234
Beta-330172	9,880 ± 40								
			Start Component 3/Feature 10.01 (upper Stratum 5)			11,589–11,215	11,371	107	11,349
Paleosol 2/Stratum 4 (Component 2)			End Paleosol 2/Stratum 4 (Component 2)			11,732–11,341	11,550	103	11,559
Beta-289378	10,020 ± 40	11,745–11,316	11,512	109	11,508	11,799–11,425	11,636	94	11,642
Beta-289377	10,080 ± 40	11,938–11,396	11,637	129	11,649	11,967–11,483	11,703	105	11,701
AA-86967/	10,120 ± 75	11,980–11,622	11,784 ^b	88	11,771	11,979–11,625	11,789	86	11,774
UCIAMS-71260	10,125 ± 20								
AA-86966	10,290 ± 75	12,395–11,773	12,083	172	12,075	12,392–11,774	12,081	167	12,073
AA-86965	10,295 ± 60	12,388–11,825	12,102	149	12,089	12,387–11,826	12,099	147	12,087
AA-86961	10,330 ± 70	12,514–11,832	12,179	148	12,179	12,419–11,834	12,173	144	12,173
AA-86963	10,340 ± 75	12,518–11,835	12,188	150	12,190	12,425–11,832	12,180	145	12,182
AA-86962	10,355 ± 60	12,417–11,983	12,216	123	12,216	12,411–11,992	12,211	120	12,211
AA-86960	10,415 ± 60	12,530–12,069	12,290	125	12,288	12,520–12,058	12,271	117	12,270
AA-86964	10,420 ± 60	12,532–12,081	12,299	124	12,297	12,520–12,071	12,280	115	12,278
AA-86968/	10,440 ± 60	12,545–12,249	12,457 ^c	66	12,471	12,542–12,123	12,415	93	12,428
UCIAMS-71261	10,485 ± 25								
			Start Paleosol 2/Stratum 4			12,743–12,285	12,518	103	12,513
Paleosol 1/Substratum 2b (Component 1)			End Paleosol 1/Substratum 2b/Component 1			13,044–12,520	12,798	140	12,814
AA-86969	11,060 ± 60	13,067–12,773	12,917	78	12,919	13,075–12,800	12,942	75	12,950
Beta-11209	11,340 ± 150	13,473–12,865	13,197	146	13,198	13,377–12,809	13,093	146	13,095
			Start Paleosol 1/Substratum 2b/Component 1			14,227–12,814	13,350	423	13,243

^a $\chi^2 = 2.5$; $df = 1$; $T_{crit} = 3.8$.
^b $\chi^2 = 0.0$; $df = 1$; $T_{crit} = 3.8$.
^c $\chi^2 = 0.4$; $df = 1$; $T_{crit} = 3.8$.

applied a Bayesian stratigraphic model in the OxCal v4.3.2 Bronk Ramsey (2017) program and the r:5 IntCal13 atmospheric curve (Reimer et al., 2013) when calibrating dates to better evaluate the time of deposition of the stratigraphic profile as well as estimate ages of Components 1, 2, and 3 (Figure 5). We modeled four *phases* of deposition: Paleosol 1/Stratum 2b containing Component 1, Paleosol 2/Stratum 4 containing Component 2, Component 3, and middle-upper Stratum 6. Unfortunately we did not find enough preserved

charcoal to date Stratum 2a, Stratum 3, most of Stratum 5, and lowermost Stratum 6, so we could not model the depositional rates for the entire profile; however, we can discuss these unmodeled depositional events in terms of the time between dated events. Each depositional phase was constrained by *boundaries* to approximate the beginning and end of depositional phases. Additionally, in the model we used the *combine* command to average three sets of paired dates, two sets consisting of split samples dated by two labs, and one set

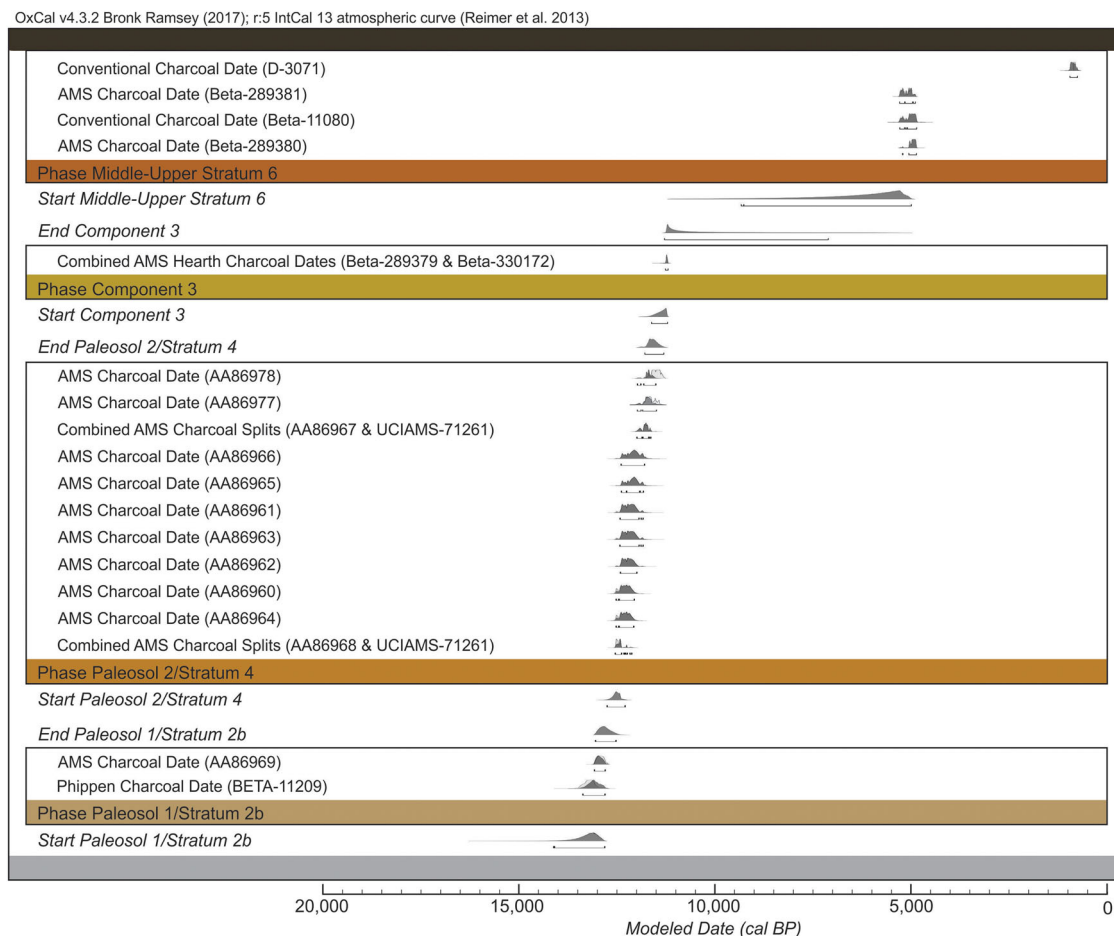


FIGURE 5 Calibrated and modeled radiocarbon dates from Owl Ridge [Color figure can be viewed at wileyonlinelibrary.com]

consisting of two dates from the F10.01 hearth feature (see Table 2 for χ^2 results). Agreement indices indicate good agreement between unmodeled (prior) and modeled (posterior) calibrated ranges in which $A_{\text{model}} = 89.9\%$ and $A_{\text{overall}} = 90.4\%$.

The modeled 2σ calibrated age range for Paleosol 1 in Stratum 2b is 13,377–12,800 cal yr BP, suggesting as much as a 577-cal-yr time span for development of Paleosol 1 and time frame for deposition of Component 1 artifacts. The modeled age range for Paleosol 2 in Stratum 4 is 12,542–11,425 cal yr BP, suggesting a potential 1,117-cal-yr time span for development of Paleosol 2 and time frame for deposition of Component 2 artifacts. The modeled age range for Component 3 is 11,267–11,201 cal yr BP, suggesting a 66-cal-yr time span for deposition of Component 3 artifacts and feature F10.01. The modeled age range of the middle-upper section of Stratum 6 is 5,211–742 cal yr BP, providing a 4,469-cal-yr time span for deposition of middle-upper Stratum 6. When examining the 2σ age ranges for both prior and posterior dates, there is as much as 952 calendar years of chronological separation between the youngest Component 1 date and oldest Component 2 date. There is as much as 598 years of separation between Components 2 and 3. Our dating results indicate the site was visited three times during about 2,000 years, twice during the late Pleistocene and once during the earliest Holocene.

4.3 | Particle-size distributions and site formation

Ten discrete sediment samples collected from the late Pleistocene and Holocene-aged deposits in the main excavation block were analyzed for particle-size distributions. Strata 1, 4, and 5 were each sampled twice, with a lower and upper subsample each taken from Strata 1 and 4, and a lower and middle subsample taken from Stratum 5. Strata 2a, 2b, 3, and 6 were each sampled once. Both Stratum 1 subsamples contain >30% (lower is 39% and upper is 44%, respectively) coarse-fraction sediment with clasts ranging in size from very fine gravels (2–4 mm) to very small boulders (64–128 mm). In contrast, the deposits above Stratum 1 overwhelmingly consist of fine-fraction sediment. In fact, samples from the lower portion of the profile, Strata 2a, 2b, and 3, had 0% coarse fraction. Most of the remaining samples from the upper portion of the profile contained 2% or less coarse fraction, with these clasts falling into the very fine gravel size subfraction. The sample from the middle bed of Stratum 5, however, contained 8% coarse fraction with 5% very fine gravel and 3% clasts larger than 4 mm in diameter.

Particle-size distributions of the fine fraction generally confirm field observations. Stratum 1 was described in the field as bedded gravelly sands. Fine-fraction sediment from Stratum 1 lower and upper

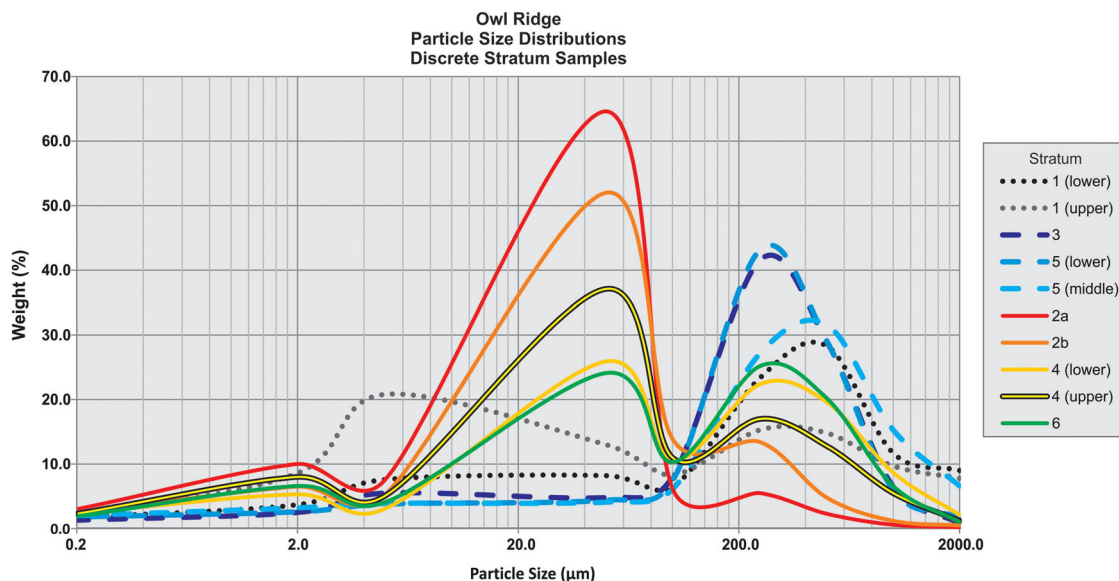


FIGURE 6 Particle-size distribution data from discrete stratum samples described in the text [Color figure can be viewed at wileyonlinelibrary.com]

subsamples is dominated by sand (79% and 56%, respectively), with 16–34% silt and 5–10% clay. Both samples are characterized as loamy sands with a considerable amount of gravel-sized and larger clasts, as noted above. The strata (2a, 2b, 4, and 6) described in the field as silts and sandy silts have sand contents of 15–63%, silt contents of 28–72%, and clay contents of 8–13%. Particle-size distributions indicate that Strata 2a and 2b are both silt loams. The lower subsample of Stratum 4 is sandy loam, and the upper Stratum 4 subsample is loam. The Stratum 6 sample is a fine sandy loam. Strata 3 and 5 were field identified as sands. Indeed they both have high sand contents of 86–87% as opposed to silt contents of 8–10% and clay contents of 4–5%. Particle-size distributions indicate that Stratum 3 is loamy sand, middle Stratum 5 is loamy sand, and lower Stratum 5 is sand.

A closer examination of subfractions of sediment fines illustrates a few key patterns obscured by a simple trigon-based sediment classification scheme (Figure 6). The lower Stratum 1 sample is unimodal in its distribution, dominated by medium sands with little silt and clay present. The upper sample has more of a bimodal distribution with modes in fine silt and medium-to-fine sands, signaling a fining-upward sequence in Stratum 1. This, together with the preponderance of gravel-size and larger clasts, provides support of Stratum 1 as an alluvial deposit.

Strata 2a, 2b, 4 (lower and upper samples), and 6 are similar to each other with peaks in the coarse-to-medium silt fraction (50–5 μm), which includes the characteristic loess fraction (50–20 μm), suggesting that a specific dust-dominated eolian depositional process, for example, loess storms, contributed to deposition of these layers. Still, there are key differences between these strata that support the varied field designations. Strata 2b, 4, and 6 were characterized as sandy silts in the field. These samples express a bimodal distribution with modes in both the loess fraction and medium-to-fine sand (500–100 μm) fraction. In contrast, Stratum 2a, characterized as silt in the field, presents a strong primary mode in the loess fraction, with a weak, secondary mode in the coarse-to-medium clay fraction. Stratum 2b is the only sample in

the entire profile that can be characterized as a true loess based on particle-size distributions. It consists of 57% silt (comprised of >50% loess fraction), 34% sand, and 9% clay. The others either have too much silt (2a) or too much sand (4 and 6), but certainly they are still loess-like, falling within the range of loess-deposit variability identified previously in central Alaska (Muhs & Budahn, 2006; Muhs et al., 2013). The higher percentages of sand in Stratum 4 (63% in lower and 48% in upper) and Stratum 6 (63%) provide evidence of stronger or at least more gusty winds at the site that could have entrained these coarser materials during deposition from a nearby source, in combination with loess that traveled from a more distant source. The finer sediment in Stratum 2, especially in Stratum 2a, indicates perhaps weaker or more constant winds that entrained almost exclusively sediment from a distant source.

Strata 3 and 5 expressed very similar distributions with only slight differences. Stratum 3 and the lower sample from Stratum 5 have nearly the same particle-size distributions that vary inversely with the Stratum 2a sample. Notably, they are unimodal in fine sands, which is slightly different from the distribution of middle Stratum 5. This sample is unimodal in medium sands. As noted in the field, the middle bed of Stratum 5 is coarser in texture than the lower bed and also contains gravel-sized clasts. The sands of Stratum 3 and perhaps those found in the lowest portion of Stratum 5 were deposited primarily though eolian deposition from a nearby source, likely from the terrace riser just below the site. Given the presentation of the field data from the site and from the GTUs discussed above, we argue that Stratum 5 primarily represents a series of overland flow deposits, colluvium that originated from several hundred meters upslope of the Owl Ridge site.

4.4 | Lithic artifacts and site formation

4.4.1 | Character of the lithic assemblages

In total we found 3,319 lithic artifacts during our excavations in 2007, 2009, and 2010. Of these, 791 are assigned to Component 1, 506 to

TABLE 3 Major artifact classes and types by cultural component from the 2007–2010 excavations at Owl Ridge

		Components			
Artifact typology	n (%)	1	2	3	Unassigned
Cores					
Tested cobbles	9 (0.3%)	1 (0.1%)	4 (0.8%)	4 (0.2%)	0 (0.0%)
Flake cores	4 (0.1%)	0 (0.0%)	2 (0.4%)	2 (0.1%)	0 (0.0%)
Subtotal	13 (0.4%)	1 (0.1%)	6 (1.2%)	6 (0.3%)	0 (0.0%)
Debitage					
Angular shatter	95 (2.8%)	9 (1.1%)	13 (2.6%)	71 (3.9%)	2 (0.9%)
Cortical spalls	518 (15.6%)	87 (11.0%)	56 (11.1%)	358 (19.9%)	17 (7.5%)
Flakes	2,042 (61.5%)	492 (62.2%)	283 (55.9%)	1,113 (62.0%)	154 (68.1%)
Blade-like flakes	6 (0.2%)	1 (0.1%)	3 (0.6%)	2 (0.1%)	0 (0.0%)
Resharpener chips	364 (11.0%)	110 (13.9%)	64 (12.6%)	154 (8.6%)	36 (15.9%)
Biface thinning flakes	224 (6.7%)	68 (8.6%)	66 (13.0%)	77 (4.3%)	13 (5.8%)
Burin spalls	1 (<0.1%)	0 (0.0%)	1 (0.2%)	0 (0.0%)	0 (0.0%)
Microblades	4 (0.1%)	0 (0.0%)	1 (0.2%)	1 (<0.1%)	2 (0.9%)
Technical spalls	1 (<0.1%)	0 (0.0%)	0 (0.0%)	1 (<0.1%)	0 (0.0%)
Subtotal	3,255 (98.1%)	767 (97.0%)	487 (96.2%)	1,777 (98.9%)	224 (99.1%)
Tools					
Concave-based points	1 (<0.1%)	0 (0.0%)	1 (0.2%)	0 (0.0%)	0 (0.0%)
Lanceolate points	1 (<0.1%)	0 (0.0%)	1 (0.2%)	0 (0.0%)	0 (0.0%)
Triangular points	3 (<0.1%)	3 (0.4%)	0 (0.0%)	0 (0.0%)	0 (0.0%)
Point tips	2 (<0.1%)	1 (0.1%)	1 (0.2%)	0 (0.0%)	0 (0.0%)
Bifaces	17 (0.5%)	11 (1.4%)	4 (0.6%)	2 (0.2%)	0 (0.0%)
Side scrapers	4 (0.1%)	0 (0.0%)	1 (0.2%)	1 (<0.1%)	2 (0.9%)
End scrapers	2 (<0.1%)	0 (0.0%)	1 (0.2%)	1 (<0.1%)	0 (0.0%)
Combination tools	1 (<0.1%)	0 (0.0%)	0 (0.0%)	1 (<0.1%)	0 (0.0%)
Retouched flakes	15 (0.5%)	7 (0.9%)	3 (0.6%)	5 (0.3%)	0 (0.0%)
Cobble chopper	1 (<0.1%)	0 (0.0%)	0 (0.0%)	1 (<0.1%)	0 (0.0%)
Anvil stone	1 (<0.1%)	1 (0.1%)	0 (0.0%)	0 (0.0%)	0 (0.0%)
Hammer stone	3 (<0.1%)	0 (0.0%)	1 (0.2%)	2 (0.1%)	0 (0.0%)
Subtotal	51 (1.5%)	23 (2.9%)	13 (2.6%)	13 (0.8%)	2 (0.9%)
Component totals		791 (100%)	506 (100%)	1796 (100%)	226 (100%)
Assemblage totals		791 (23.8%)	506 (15.3%)	1796 (54.1%)	226 (6.8%)

Component 2, and 1,796 to Component 3 (Table 3). A total of 226 artifacts could not be confidently assigned to a component because they were found in the N83 squares along the edge of the terrace where stratigraphic units 4–6 were difficult to tease apart (Figure 4). Though lithic artifact-tool numbers recovered in our excavations are few, we found several diagnostic pieces (Figure 7). In Component 1 we found fragments of at least three ultra-thin, triangular-shaped, bifacially worked projectile points. Though other artifact types commonly associated with the Nenana technocomplex are not present, the toolkit is consistent with this designation (cf., Goebel et al., 1991; Hoffecker et al., 1993). In Component 2 we obtained at least three more robustly made bifacial projectile points, one that is lanceolate-shaped; one that is heavily

reworked, slightly shouldered, and concave-based; and one point tip. We also found one probable microblade but no microblade cores or technical spalls (e.g., core tablets, platform rejuvenation spalls, or frontal rejuvenation spalls), albeit previous investigations found two more microblades and two “technical spalls.” Given these diagnostic artifacts, Component 2 is consistent with a Denali technocomplex affiliation (cf., West, 1967). In Component 3 we found no projectile points; however, we found one microblade and one technical spall (specifically a frontal rejuvenation spall) related to wedge-shaped microblade core reduction; therefore, it is consistent with a Denali technocomplex assignment. Raw materials are dominated by cherts and several types of fine-grained volcanic rocks such as basalt, rhyolite, and andesite (Table 4). The

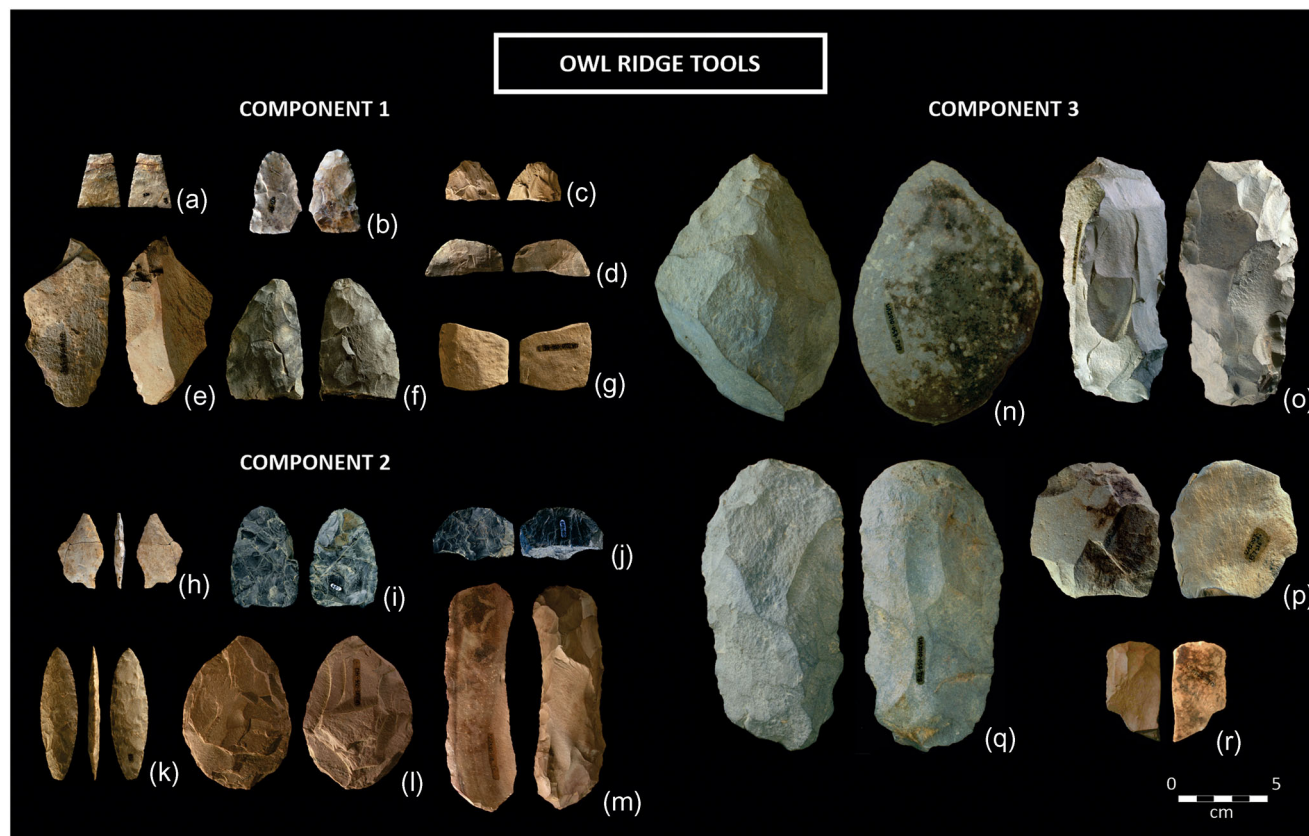


FIGURE 7 Owl Ridge tools by component found during the 2007–2010 excavations: (a) triangular-shaped point, (b) point preform, (c–d, f) bifaces, (e) retouched flake, (g) scraper fragment, (h) concave-based point, (i, l) bifaces, (j) retouched flake, (k) lanceolate point, (m) double end scraper, (n) cobble-spall scraper, (o–q) bifaces, (p) retouched flake, (r) end scraper (adapted from Gore & Graf, 2018) [Color figure can be viewed at wileyonlinelibrary.com]

composition of raw materials changes through time with andesite becoming increasingly more prevalent and economically important (Gore & Graf, 2018).

4.4.2 | Artifact plunge and trend

To examine orientation and displacement of artifacts in each component, artifact plunge was scored on 355 in situ artifacts (Figure 8). Artifacts with plunge measurements greater than 45° are more likely to have experienced significant postdepositional

movement in the profile through freeze-thaw action (Johnson & Hansen, 1974; Schweger, 1985; Wood & Johnson, 1978). Though all three components have a few artifacts with >45° plunges, the distribution of plunge measurements skewed positively toward smaller plunge degrees with means of 24° for Component 1, 16° for Component 2, and 17° for Component 3. In fact, more than 80% of artifact plunges in all three components were less than 45° so that most artifacts were lying closer to horizontal than vertical with no significant difference between assemblages (Kruskal-Wallis *H* statistic = 3.409, 2 *df*, *p* = .182). Artifact trend

TABLE 4 Major raw material classes by cultural component from the 2007–2010 excavations at Owl Ridge

Raw materials	<i>n</i> (%)	Components			Unassigned
		1	2	3	
Chert	1209 (36.4%)	488 (61.7%)	435 (86.0%)	145 (8.1%)	141 (62.4%)
Basalt	291 (8.8%)	36 (4.6%)	12 (2.4%)	243 (13.5%)	0 (0.0%)
Rhyolite	48 (1.4%)	2 (0.3%)	0 (0.0%)	45 (2.5%)	1 (0.4%)
Andesite	1592 (48.0%)	247 (31.2%)	28 (5.5%)	1239 (69.0%)	78 (34.5%)
Other	179 (5.4%)	18 (2.3%)	31 (6.1%)	124 (6.9%)	6 (2.7%)
<i>Component totals</i>		791 (100%)	506 (100%)	1796 (100%)	226 (100%)
<i>Assemblage totals</i>	3319 (100%)	787 (23.8%)	506 (15.3%)	1796 (54.1%)	226 (6.8%)

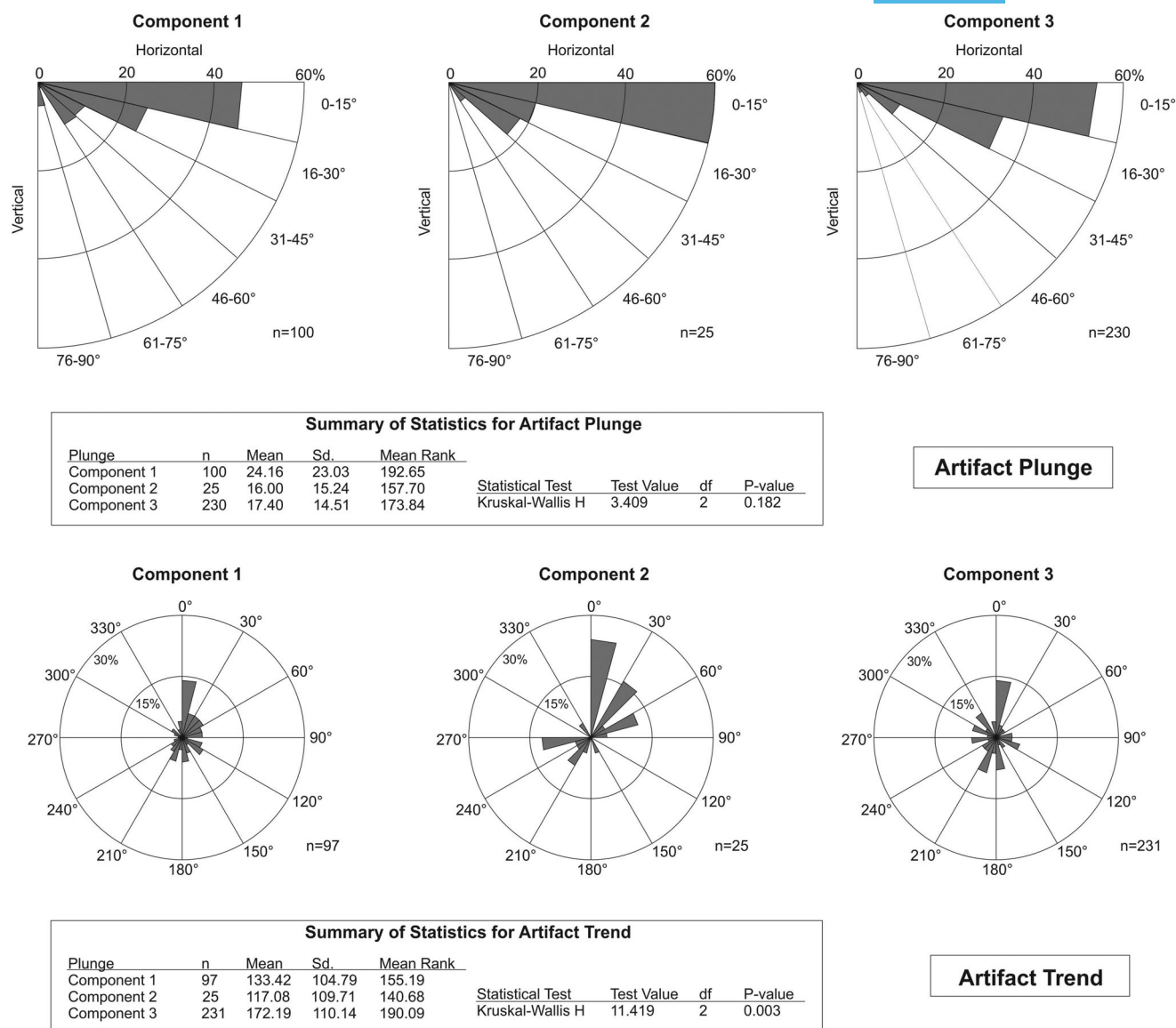


FIGURE 8 Artifact plunge and trend, showing corresponding statistics discussed in the text

was confidently recorded for 353 of the 355 artifacts for which plunge was recorded.

Artifact trends in Component 1 indicate mostly a northeast orientation. Trends for Component 2 express both a northeast and southwest orientation. Trends for Component 3, however, appear random with no obvious orientation pattern. The distributions of component trend measurements are not statistically the same (Kuskal-Wallis H statistic = 11.419, 2 df , $p = .003$), indicating that the three component assemblages may have been affected by different postdepositional processes. Though the patterns of Components 1 and 2 are slightly different, both sets of trends run mostly parallel to the slope of the site and in both northern and southern directions, which may indicate some minor movement due to solifluction of annually thawing sediment near permafrost level. Indeed both field and lab observations indicate some minor cryoturbation in the components' respective stratigraphic units, Stratum 2 and Stratum 4 (DiPietro et al., in review). The stochastic pattern of Component 3, on

the other hand, indicates artifacts may be still positioned relatively close to where humans left them behind. It also suggests these materials were discarded at the site near the end of deposition of Stratum 5, and not transported far downslope by colluvial activity.

4.4.3 | Artifact refits

One of us conducted a refit analysis of the entire Owl Ridge assemblage (Melton, 2015), finding a total of 119 refits, 32 within Component 1, 17 within Component 2, and 69 within Component 3 (Figure 9). There were no cross-component refits except for one found in the compressed area at the terrace edge (N83E105–106). One refit was between an artifact found in situ in Component 2 (in N85E104) and one found on the surface near the terrace edge (N84E106) where Phippen (1988) screened during his testing project. Within each component, refits displayed horizontal movement in multiple directions and between activity areas.

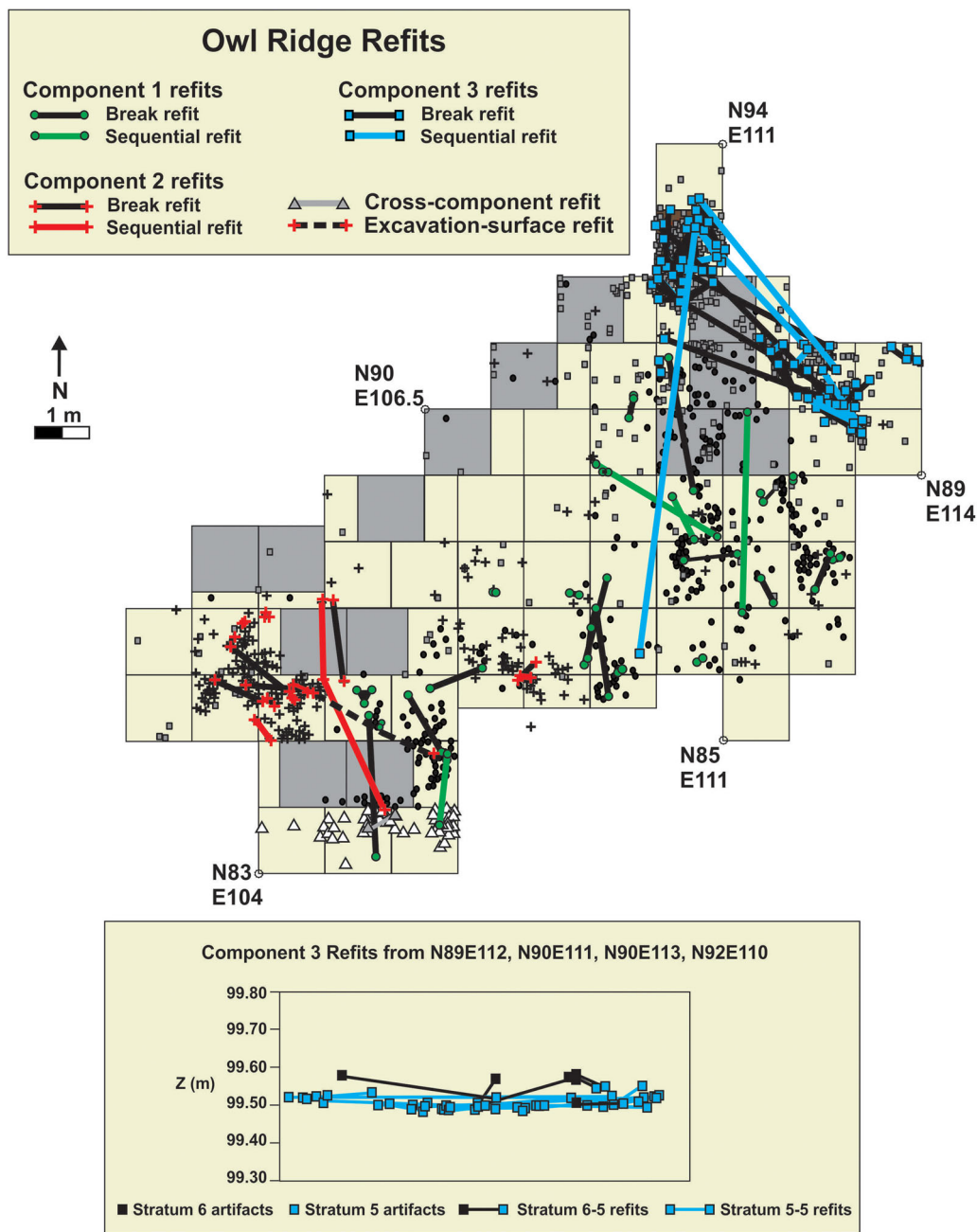


FIGURE 9 Horizontal and vertical refits of artifacts from the main block excavation. Note the location of the cross-component refit and refit between an artifact from our excavation and one found on the surface where Phippen's 1980s backdirt pile was positioned on the site surface [Color figure can be viewed at wileyonlinelibrary.com]

As mentioned above in the stratigraphy section, during excavation we combined all artifacts we found in uppermost Stratum 5 ($n = 971$), at the Stratum 5/6 contact ($n = 480$), and in Stratum 6 ($n = 345$) as Component 3. Where we found materials in Stratum 6, they were much fewer in number compared with Stratum 5 and the contact between the two layers. Moreover, the majority of artifacts found in Stratum 6 were made on andesite, the dominant raw material of Stratum 5. Following fieldwork, we wanted to better understand how artifacts from upper Stratum 5 related to lowermost Stratum 6. Were all of these materials really

part of Component 3 or did they represent two different components? Refitting informed on this question. Five of the Component 3 refits crossed the stratigraphic boundary in which each of the five was identified between a piece found in Stratum 5 and one found in Stratum 6. Given refits between Stratum 5 and Stratum 6, our field observations are upheld; the materials from uppermost Stratum 5 and lowermost Stratum 6 are part of the same cultural component. This is also supported by the observation that the stratigraphic boundary between Stratum 5 and 6 was gradual and not abrupt.

5 | DISCUSSION

Below we discuss the varied field and lab geoarchaeological results presented above to address several key research contexts related to the goals of our project at Owl Ridge.

5.1 | Owl Ridge depositional history and geological integrity

The Owl Ridge stratigraphic profile comprises a set of unconsolidated fine-grained sediments mantling an ancient glaciofluvial terrace of the Teklanika River. The stratigraphic sequence is as follows. At the base of the profile, Stratum 1 represents glacial outwash from the Healy glacial event, dating to early MIS-3 (Dortch et al., 2010; Warhaftig, 1958). Based on our observations from both site stratigraphy and particle-size-distribution data, Stratum 2 represents a loess deposit (Loess 1), newly subdivided into a lower gleyed silt (Stratum 2a) and an upper sandy silt (Stratum 2b) with redox features. Stratum 2a represents the current permafrost level with gleying from being perennially reduced in a humid frozen environment. Though we report no dates from this section of Loess 1, its character is very similar to the lowermost loess deposits at two sites in the nearby Nenana Valley, Dry Creek and Panguingue Creek, with lowermost gleyed silt deposits resting unconformably on ancient glacial alluvium and dated to ~16,000–13,000 cal yr BP (Goebel & Bigelow, 1992, 1996; Graf et al., 2015; Hoffecker et al., 1996). The redox features that characterize overlying Stratum 2b represent alternating periods of complete thawing and complete drying of sediment after deposition, and the weakly expressed Paleosol 1 present near the top of Stratum 2b indicates a brief cessation of eolian deposition with ground stabilization when humans first visited Owl Ridge. Pieces of willow charcoal provide an age range of about 13,380–12,800 cal yr BP for the paleosol and Component 1. Currently, Component 1 at the Owl Ridge site is the oldest in the Teklanika Valley and represents a Nenana complex occupation. Recent work at the Teklanika West site provided two radiocarbon dates on bison bone of 13,070–12,700 cal yr BP; however, these were found in a compressed context along with two additional bison bone dates ranging from 11,250–9700 cal yr BP and artifacts ascribable to the Denali technocomplex (Coffman, 2011).

Next, Stratum 3 is a cliffhead sand deposit (Sand 1) that thins away from the terrace edge toward the apex of the ridge, representing less stable surface conditions. Indeed humans were not present at Owl Ridge at this time. Though not directly dated, modeled boundary ages of the bracketing Strata (2b and 4) as well as the modeled age ranges, weighted means, and medians for the youngest and oldest dates of these two layers, indicate Stratum 3 formed in about 500 years between about 13,000 cal yr BP and 12,500 cal yr BP. Similarities in thickness, lateral extent, particle size, and age indicate that Sand 1 at Owl Ridge corresponds to Sand 1 at other nearby sites resting on Healy aged glacial terraces in the Nenana Valley, including Dry Creek, Walker Road, and Little

Panguingue Creek (Goebel, Powers, Bigelow, & Higgs, 1996; Gómez Coutouly et al., 2019; Graf et al., 2017; Powers et al., 2017).

Stratum 4 represents a return to more gentle loess deposition (Loess 2). It preserves a moderately expressed Paleosol 2 representing land-surface stabilization when humans revisited the site. Linear redox features near the base of the stratum may indicate that at some point in time the local permafrost layer was at this position in the profile. Minor postdepositional solifluction affected the stratum, leading to small involutions that moved materials 1–15 cm from their original positions within, but not outside, the stratum. Willow charcoal was abundant, dating Paleosol 2 to about 12,540–11,430 cal yr BP and providing Component 2 with a Denali-complex chronological association.

Stratum 5 is a relatively thick set of overland flow deposits (Colluvium 1) that thin toward the terrace edge. It preserves neither paleosols nor wood charcoal, except for the few willow-charcoal pieces associated with the Component 3 hearth and artifacts positioned in its uppermost lens near the contact with overlying Stratum 6. The age of the hearth and Component 3 is about 11,270–11,200 cal yr BP, providing a Denali-complex chronological association. Most of Stratum 5 (as much as 40 cm of deposit), therefore, formed in just 500 years between about 11,700 cal yr BP and 11,200 cal yr BP, representing rapid deposition of overland deposits on the site during the first few centuries of the Holocene. At the Panguingue Creek site a similarly thick colluvial package is positioned immediately below a cultural component dating to ~11,400–11,200 cal yr BP (Goebel & Bigelow, 1992, 1996).

Stratum 6 represents a shift back to eolian loess deposition (Loess 3). The deposit expresses spodosol development concurrent with deposition in the form of a well-developed B horizon with observable signs of sesquioxide translocation immediately below a well-developed O/A/E-soil-horizon sequence. Spruce charcoal samples from the middle-upper sections of the stratum provide middle-late Holocene ages (~5,200–740 cal yr BP). One sample came from the lower section of Stratum 6; however, as presented above it likely represents spruce root burn.

Based on field observations, radiocarbon dating, and particle-size data, we have documented the depositional history and geological integrity of the site. The site consists of six independently formed, alternating depositional events as discussed above. There are clearly defined boundaries between stratigraphic layers, chronological data support this sequence of events, and there is a clear vertical and chronological separation between archaeological components. Additionally, we have recognized Sand 1 as a regional chronostratigraphic marker, its character and association with underlying and overlying loess deposits being repeated at other sites in the region as suggested by Bigelow et al. (1990). At Owl Ridge we provide chronological control with dates from the bracketing loess deposits placing this regional depositional event during the first 500 years of the Younger Dryas global chronozone similar to Dry Creek (Graf et al., 2015). The subsequent colluvial event at Owl Ridge corresponds to one found at nearby Panguingue Creek, dating to the first few centuries of the early Holocene. It may thus represent a regional chronostratigraphic marker expected in specific contexts

where there was a potential upslope source for such colluvial deposition. With these two cases, we now have evidence of an earliest Holocene-aged colluvial deposit, which, in concordance with previous Nenana Valley stratigraphic nomenclature, we propose the designation "Colluvium 1." With regard to the question of source material for eolian sediment at these interior Alaskan sites, it is difficult to directly test the hypothesis that sand deposits originated from southern winds and loess deposits originated from more northern and eastern winds (DiPietro et al., 2017). The data presented here; however, do not refute this assumption. The Stratum 3 cliffhead sands originated from winds blowing south-to-north, down the Teklanika Valley. Stratum 3 is thickest near the southern terrace edge, with the immediate sediment source being located immediately below the site on the southern terrace riser, whereas loess deposits blanket the site in more-or-less uniform thickness and could have originated from the north and east or the south. Certainly, they do not follow the same depositional pattern as the sand.

5.2 | More on site formation

Other variables informing on site formation and integrity of site deposits come from the artifact assemblages representing Components 1, 2, and 3. Taking both refits and plunge and trend data together, it appears that displaced artifacts occur minimally at Owl Ridge. Artifact plunge and trend data demonstrate artifacts moved little in the site after deposition. Plunges are overwhelmingly resting in a nearly horizontal position for all three components. Trends show perhaps a little more postdepositional movement occurred in Components 1 and 2 than in Component 3. Despite trend data indicating some movement of artifacts in Components 1 and 2, plunge data signal minimal displacement. Likewise, refit analysis points to minimal vertical movement in these components. These data also reveal Component 3 was deposited after the major colluvial events of Stratum 5, as the depositional environment was shifting back to one dominated by eolian deposition. Perhaps a stratigraphic designation for all Component 3 artifacts should be the Stratum 5/6 contact, literally occurring at the transition between two depositional regimes.

Detailed spatial analyses of lithic assemblages are presented elsewhere (Puckett & Graf, in review), but even cursory examination of Figure 2 illustrates activity areas of the three components do not directly overlap across space. Discrete areas suggest people used the site differently through time, supporting the independent nature of the accumulation of each as separate behavioral depositional events. Further, the patterning of horizontal refits within each component indicates that components represent three single occupation events.

Here we presented basic numbers of the lithic assemblages so the reader can understand the behavioral context of the components; however, a more detailed analysis of the lithic technological organization of site assemblages is presented elsewhere (Gore & Graf, 2018). Nevertheless, a recap of that paper is illustrative here. Despite the site functioning as a short-term camp through time, Gore & Graf (2018) found significant behavioral differences between components. During the Component 1 occupation, hunters stayed for

very short visits to hunt. They brought a Nenana-complex hunting toolkit with Chindadn-type projectile points and several bifaces, but no unifacial processing tools. Debitage and raw-material data indicate they retooled at Owl Ridge with local raw materials. During the Component 2 occupation, hunters brought lanceolate projectile points as well as processing tools, representing a Denali-complex hunting and processing toolkit. They used both local and nonlocal raw materials. During the Component 3 occupation occupants left behind mostly a processing toolkit with no projectile points. The characters of artifact assemblages from the three components indicate inhabitants became increasingly familiar with the site and its environments through time.

5.3 | Paleoclimatic and environmental conditions at Owl Ridge and potential effects on humans

Depositional history of the unconsolidated sediments comprising the archaeological record (Strata 2–6) at Owl Ridge indicates an exclusively eolian depositional regime from at least 14,000 cal yr BP to about 11,700 cal yr BP. Next, the site experienced a very brief period of rapid accumulation of colluvium lasting about 500 years. Then, by about 11,200 cal yr BP, the site experienced a switch back to an eolian depositional regime. The eolian-dominated depositional environment suggests that through time this location experienced relatively dry conditions with brief periods of increased windiness indicated by occasional spikes in the sand (e.g., Sand 1 and minor peaks in the sand fraction of loess units). The two paleosols in the late Pleistocene section, Paleosol 1 and Paleosol 2, signal periods of stability at 13,380–12,800 cal yr BP and 12,540–11,430 cal yr BP, with minimal depositional activity and likely milder climatic conditions than the prevailing windy, dry conditions of the terminal Pleistocene (Guthrie 2001; Schweger, Matthews, Hopkins, & Young, 1982). The dominant pattern of eolian deposition was interrupted by rapid deposition of thick colluvium immediately following the development of Paleosol 2 and before the Component 3 occupation event, so between ~11,430 cal yr BP and 11,270 cal yr BP. Colluvium 1 indicates a very brief interval of increased precipitation at the beginning of the early Holocene when colluvial sediment moved downslope from either melting snow or summer rains. It also signals low vegetation cover at this time.

The site preserved minimal paleobotanical data; however, we know the region experienced light vegetation cover throughout the terminal Pleistocene until trees—*Populus* and eventually spruce—migrated into the North Alaska Range after 11,000 cal yr BP (Bigelow & Powers, 2001; Tinner et al., 2006). The natural charcoal, as well as charcoal procured by humans for a hearth fire, can shed some light on local conditions. These pieces were exclusively willow before 11,000 cal yr BP and exclusively spruce afterward. This suggests that during the terminal Pleistocene, willow was readily present at or near the site, especially during the latter half of the Allerød interval and throughout the Younger Dryas. Few pieces of charcoal were found in Paleosol 1, and observing no charcoal below this layer supports inferences from

the regional pollen records of a pre-14,000 cal yr BP herb-tundra biome and transition to a willow and birch shrub-tundra during the Allerød interstadial (Anderson et al. 2004; Bigelow & Powers, 2001). We may expect humans procured wood with the greatest utility to provide the fire for warmth, cooking, and as an insect repellent. That inhabitants of Component 3 selected willow indicates that by 11,200 cal yr BP larger woody species (i.e., *Populus* or spruce trees) were not yet available at or near the site. Certainly, by 5,200 cal yr BP spruce was growing at Owl Ridge, but we suspect that it may have been present three-to-five millennia before that date, given the presence of spodic signatures throughout Stratum 6 and regional pollen records referenced above. Field observations of soil formation in Stratum 6 indicate the site was fully treed with spruce and other boreal forest species through much of its deposition. We do note that the increase in sand in this stratum suggests windy periods through the Holocene.

Humans first used the Owl Ridge location sometime between 13,380–12,800 cal yr BP, at the end of the Allerød interstadial as shrub-tundra emerged across the interior of Alaska. They must have found the location a good place for a hunting camp and to keep watch for fauna traveling through the valley. Component 2 occupants used the site at 12,540–11,430 cal yr BP, during the final centuries of the Younger Dryas chronozone. The presence of Sand 1, the chronostratigraphic marker of the region's Younger Dryas climatic record, between Components 1 and 2, suggests conditions at this time were perhaps too harsh for humans at Owl Ridge. If humans did attempt to camp at the site they likely would have experienced strong winds with sand blowing up onto the site's surface. Component 3 comprises the most extensive occupation of the site at ~11,270–11,200 cal yr BP, dating to the early Holocene immediately after a regional colluvial event that piled tens of centimeters of coarse-grained sediment on the site surface due to increased precipitation over a thinly vegetated land surface.

During all three site occupations, vegetation was sparse, visibility was high, and the site's position offered an excellent overlook of the Teklanika River valley and side drainage of First Creek. Further, when people were present at Owl Ridge, environmental conditions were relatively mild. The paleosols associated with Components 1 and 2 indicate periods of less windy conditions, and the willow-wood charcoal present in these paleosols indicates shrubs were present for fuel (though we found no discernable hearth features in Components 1 and 2). Perhaps some of the charcoal-rich areas of Paleosol 2 represent human-burning activity not detectable as discrete "hearth" features during excavation. Even though no paleosol is associated with Component 3, conditions were relatively moderate following a time of either torrential rainfall or heavy snowmelt. Humans then visited the site as local climate changed from relatively heavy precipitation back to lower-energy loess deposition and drier conditions. The site seems to have been abandoned and never revisited following 11,200 cal yr BP. The boreal forest would have closed in the view from the site, making the hike up to the ridge less desirable for human foragers.

6 | CONCLUSIONS

Our work at Owl Ridge provides a glimpse at life between 13,100 cal yr BP and 11,200 cal yr BP in interior Alaska. Two of our main excavation goals were to assess site stratigraphy and geological integrity of the deposits and cultural components and to refine the emerging chronology of the site so that we could then address questions of how humans settled the region and changed their methods of making a living during the settling-in process at the Pleistocene-Holocene boundary. We found site deposits to be largely intact with clear stratigraphic integrity upheld across the site, except for within 50–80 cm of the terrace edge where layers are somewhat compressed. This compression affected only a small portion of the site's lithic assemblage. We were able to refine site chronology by obtaining, reporting, and analyzing 20 new radiocarbon dates in conjunction with previously reported dating results. We found a series of dates from within and between layers of the site to be internally consistent, providing a reliable chronological model for depositional events and the dating of human occupations. In doing this we report that the site was visited on three separate occasions within a 2,000-year period. We found stratigraphic and chronological separation between the Nenana technocomplex and Denali technocomplex at the site. This is a pattern in the greater Nenana Valley that is consistently upheld at sites with well-preserved, good internal stratigraphic records, and it is a chronological pattern that is consistently held up in well-dated Allerød, Younger Dryas, and post-Younger Dryas sites across central Alaska as well as western Beringia (i.e., the Yana-Indigirka lowlands and Kamchatka). Finally, our work at Owl Ridge provides paleoenvironmental information and informs on humans living in the region during the terminal Pleistocene and early Holocene.

Though the earliest occupation at Owl Ridge is not the earliest in interior Alaska, it does provide evidence of the initial population inhabiting the Teklanika Valley. It demonstrates an early hunting campsite with Nenana complex material that is coeval with Clovis across North America. The site also shows a switch in technological and landuse strategies that occurred during a time of regional climatic instability. This change in technology represented by the Denali complex at Owl Ridge may represent an adaptive switch in response to local effects of the Younger Dryas; however, the change could also represent two distinct populations of ancient Beringian inhabitants in Alaska during the terminal Pleistocene as predicted by recent paleogenomic studies (Moreno-Mayar, Potter, et al., 2018; Moreno-Mayar, Vinner, et al., 2018).

ACKNOWLEDGEMENTS

We would like to thank the field crews from 2009 to 2010, including Heather Smith, John Blong, Josh Keene, Angela Younie, Takako Sakamoto, Anna Gilmer, Stuart White, and Nancy Bigelow. Additional thanks to Heather Smith and Angela Younie for creating several of the graphics presented in the paper. We thank the journals anonymous reviewers for their detailed comments. We would like to acknowledge

both BCS-Archaeology and OPP-Arctic Social Sciences Programs at the National Science Foundation (awards 0917648 and 1029094) for supporting the project. The State of Alaska provided appropriate collections agreements and research permits.

CONFLICT OF INTERESTS

The authors declare that there is no conflict of interests.

ORCID

Kelly E. Graf  <http://orcid.org/0000-0003-3494-5478>

REFERENCES

- Anderson, P. M., Edwards, M. E., & Brubaker, L. B. (2004). Results and Paleoclimate Implications of 35 Years of Paleocological Research in Alaska. *Development in Quaternary Science*, 1, 427–440.
- Begét, J. E., Bigelow, N., & Powers, R. (1991). Letter to the editor. Reply to the comment of C. Waythomas and D. Kaufman. *Quaternary Research*, 36, 334–338.
- Bigelow, N., Begét, J., & Powers, R. (1990). Latest Pleistocene increase in wind intensity recorded in eolian sediments from central Alaska. *Quaternary Research*, 34, 160–168.
- Bigelow, N. H., & Powers, W. R. (2001). Climate, vegetation, and archaeology 14,000–9000 cal yr B.P. in central Alaska. *Arctic Anthropology*, 38(2), 171–195.
- Bronk Ramsey, C. (2017). Methods for summarizing radiocarbon datasets. *Radiocarbon*, 59(2), 1809–1833.
- Coffman, S. C. (2011). *Archaeology at Teklanika West (HEA-001): An upland archaeological site, central Alaska* (Unpublished M. A. Thesis). Fairbanks: Department of Anthropology, University of Alaska.
- DiPietro, L. M., Driese, S. G., Nelson, T. W., & Harvill, L. L. (2017). Variations in late Quaternary wind intensity from grain-size partitioning of loess deposits in the Nenana River valley, Alaska. *Quaternary Research*, 87, 254–274.
- DiPietro, L. M., Graf, K. E., Driese, S. G., & Stinchcomb, G. E. (in review). Microstratigraphy of Owl Ridge: A small-scale approach to site formation, soil development, and paleoenvironment at a Pleistocene-Holocene boundary site in central Alaska. *Quaternary International*, submitted October 21, 2018.
- Dortch, J. M., Owen, L. A., Caffee, M. W., Li, D., & Lowell, T. V. (2010). Beryllium-10 surface exposure dating of glacial successions in the central Alaska range. *Journal of Quaternary Science*, 25(8), 1259–1269.
- Edwards, M. E., Mock, C. J., Finney, B. P., Barber, V. A., & Bartlein, P. J. (2001). Potential analogues for paleoclimatic variations in eastern interior Alaska during the past 14,000 yr: atmospheric-circulation controls of regional temperature and moisture responses. *Quaternary Science Reviews*, 20, 189–202.
- Goebel, T., & Bigelow, N. H. (1992). The denali complex at Panguingue Creek, central Alaska. *Current Research in the Pleistocene*, 9, 15–18.
- Goebel, T., & Bigelow, N. H. (1996). Panguingue Creek. In F. H. West (Ed.), *American Beginnings: The Prehistory and Palaeoecology of Beringia* (pp. 366–371). Chicago, IL: Chicago University Press.
- Goebel, T., & Buvit, I. (Eds.). (2011a). *From the Yenisei to the Yukon: Interpreting Lithic Assemblage Variability in Late Pleistocene/Early Holocene Beringia*. College Station, TX: Texas A&M University Press.
- Goebel, T., & Buvit, I. (2011b). Introducing the archaeological record of Beringia. In T. Goebel, & I. Buvit (Eds.), *From the Yenisei to the Yukon: Interpreting Lithic Assemblage Variability in Late Pleistocene/Early Holocene Beringia* (pp. 1–30). College Station, TX: Texas A&M University Press.
- Goebel, T., Powers, R., & Bigelow, N. (1991). The Nenana complex of Alaska and Clovis origins. In R. Bonnicksen, & K. L. Turnmire (Eds.), *Clovis origins and adaptations* (pp. 49–79). Corvallis: Center for the Study of the First Americans.
- Goebel, T., Powers, W. R., Bigelow, N. H., & Higgs, A. S. (1996). Walker road. In Frederick H. West (Ed.), *American beginnings: The prehistory and palaeoecology of Beringia* (pp. 356–363). Chicago, IL: Chicago University Press.
- Goebel, T., Slobodin, S. B., & Waters, M. W. (2010). New dates from Ushki-1, Kamchatka, confirm 13,000 cal BP age for earliest Paleolithic occupation. *Journal of Archaeological Science*, 37(10), 2640–2649.
- Goebel, T., Waters, M. R., & Dikova, M. (2003). The archaeology of Ushki Lake, Kamchatka, and the Pleistocene peopling of the Americas. *Science*, 301(5632), 501–505.
- Goebel, T., Waters, M. R., & O'Rourke, D. H. (2008). The late Pleistocene dispersal of modern humans in the Americas. *Science*, 319(5869), 1497–1502.
- Gore, A. K., & Graf, K. E. (2018). Technology and human response to environmental change at the Pleistocene-Holocene boundary in eastern Beringia: A view from Owl Ridge, central Alaska. In Frédéric Sellet (Ed.), *Lithic technological organization and paleoenvironmental change* (pp. 203–234). London: Springer.
- Graf, K. E. (2008). *Uncharted territory: Late Pleistocene hunter-gatherer dispersals in the Siberian mammoth-steppe* (Unpublished Ph.D. dissertation). Reno: Department of Anthropology, University of Nevada.
- Graf, K. E. (2010). Hunter-gatherer dispersals in the mammoth-steppe: Technological provisioning and land-use in the Enisei River valley, south-central Siberia. *Journal of Archaeological Science*, 37, 210–223.
- Graf, K. E., & Bigelow, N. H. (2011). Human response to climate during the Younger Dryas chronozone in central Alaska. *Quaternary International*, 242(2), 434–451.
- Graf, K. E., & Buvit, I. (2017). Human dispersal from Siberia to Beringia: Assessing a Beringian standstill in light of the archaeological evidence. *Current Anthropology*, 58(S17), S583–S603.
- Graf, K. E., DiPietro, L. M., Krasinski, K., Culleton, B. J., Kennett, D. K., Gore, A. K., & Smith, H. L. (2017). New geoarchaeology and geochronology at Dry Creek. In Powers, W. R., Guthrie, R. D., Hoffecker, J. F., & Goebel, T. (Eds.), *Dry Creek: Archaeology and Paleoeology of a late Pleistocene Alaskan hunting camp* (pp. 219–260). College Station, TX: Texas A&M University Press.
- Graf, K. E., DiPietro, L. M., Krasinski, K. E., Gore, A. K., Smith, H. L., Culleton, B. J., ... Rhode, R. (2015). Dry Creek revisited: New excavations, radiocarbon dates, and site formation inform on the peopling of eastern Beringia. *American Antiquity*, 80(4), 671–694.
- Graf, K. E., & Goebel, T. (2009). Upper Paleolithic toolstone procurement and selection across Beringia. In B. Blades, & B. Adams (Eds.), *Lithic Materials and Paleolithic Societies* (pp. 55–77). London: Blackwell Publishers.
- Guthrie, R. D. (2001). Origin and causes of the mammoth steppe: a story of cloud cover, woolly mammal tooth pits, buckles, and inside-out Beringia. *Quaternary Science Reviews*, 20, 549–574.
- Guthrie, R. D. (2006). New carbon dates link climatic change with human colonization and Pleistocene extinctions. *Science*, 441, 207–209.
- Gómez Coutouly, Y. A. (2012). Pressure microblade industries in Pleistocene-Holocene interior Alaska: Current data and discussions. In P. M. Desrosiers (Ed.), *Emergence of pressure blade making: From origins to modern experimentation* (pp. 347–374). New York, NY: Springer.
- Gómez Coutouly, Y. A., Graf, K. E., Gore, A. K., & Goebel, T. (2019). Little Panguingue Creek: A c. 9600-Year-Old Prehistoric Knapping Workshop in the Nenana Valley, Central Alaska. *PaleoAmerica*, 5(1), 16–31. 10.1080/20555563.2019.1575575.

- Hoffecker, J. F. (1988). Applied geomorphology and archaeological survey strategy for sites of Pleistocene age: An example from central Alaska. *Journal of Archaeological Science*, 15, 683–713.
- Hoffecker, J. F., & Powers, W. R. (1996). Little Panguingue Creek. In Frederick H. West (Ed.), *American beginnings: The prehistory and palaeoecology of Beringia* (pp. 371–374). Chicago, IL: Chicago University Press.
- Hoffecker, J. F., Powers, W. R., & Goebel, T. (1993). The colonization of Beringia and the peopling of the new world. *Science*, 259, 46–53.
- Hoffecker, J. F., Powers, W. R., & Phippen, P. (1996). Owl ridge. In *American Beginnings: The Prehistory and Palaeoecology of Beringia*. In West, F. H. (Ed.) (353–355). Chicago: University of Chicago Press.
- Holmes, C. E. (2001). Tanana river valley archaeology circa 14,000 to 9000 BP. *Arctic Anthropology*, 38(2), 154–170.
- Holmes, C. E. (2011). The Beringian and transitional periods in Alaska. In T. Goebel, & I. Buvit (Eds.), *From the Yenisei to the Yukon: Interpreting lithic assemblage variability in late Pleistocene/early Holocene Beringia* (pp. 179–191). College Station, TX: Texas A&M University Press.
- Hua, Q., Barbetti, M., Find, D., Kaiser, K. F., Friedrich, M., Kromer, B., ... Bertuch, F. (2009). Atmospheric ^{14}C variations derived from tree rings during the early Younger Dryas. *Quaternary Science Reviews*, 28, 2982–2990.
- Johnson, D. L., & Hansen, K. L. (1974). The effects of frost-heaving on objects in soils. *Plains Anthropologist*, 19, 81–98.
- Jull, A. J. T., Donahue, D. J., & Zabel, T. H. (1983). Target preparation for radiocarbon dating by tandem accelerator mass spectrometry. *Nuclear Instruments and Methods in Physics Research*, 218, 509–514.
- Kilmer, V. J., & Alexander, L. T. (1949). Methods of making mechanical analysis of soils. *Soil Science*, 68, 15–24.
- Melton, J. A. (2015). *Pieces to a puzzle: A lithic refit study evaluating stratigraphic and lithic components of the Owl Ridge site, Central Alaska* (An Undergraduate Research Scholar Thesis, Honors Program). College Station, TX: Texas A&M University.
- Moreno-Mayar, J. V., Potter, B. A., Vinner, L., Steinrücken, M., Rasmussen, S., Terhorst, J., ... Willerslev, E. (2018). Terminal Pleistocene Alaskan genome reveals first founding population of Native Americans. *Nature*, 553, 203–207.
- Moreno-Mayar, J. V., Vinner, L., de Barros Damgaard, M. P., de la Fuente, C., Chan, J., Spence, J. P., ... Willerslev, E. (2018). Early humans dispersals within the Americas. *Science*, 362(6419), eaav2621. <https://doi.org/10.1126/science.aav2621>
- Muhs, D. R., & Budahn, J. R. (2006). Geochemical evidence for the origins of late Quaternary loess in central Alaska. *Canadian Journal of Earth Sciences*, 43(3), 323–337.
- Muhs, D. R., Budahn, J. R., McGeehin, J. P., Bettis, E. A., III, Skipp, G., Paces, J. B., & Wheeler, E. E. (2013). Loess origin, transport, and deposition over the past 10,000 years, Wrangell-St. Elias National Park, Alaska. *Aeolian Research*, 11, 85–99.
- Phippen, P. G. (1988). *Archaeology at Owl Ridge: A Pleistocene-Holocene boundary age site in central Alaska* (Unpublished M.A. Thesis). Fairbanks: Department of Anthropology, University of Alaska.
- Pitulko, V. V., Nikolsky, P. A., Giry, E. Y., Basilyan, A. E., Tumskey, V. E., Koulakov, S. A., ... Anisimov, M. A. (2004). The Yana RHS site: Humans in the Arctic before the last glacial maximum. *Science*, 303(5654), 52–56.
- Pitulko, V. V., Pavlova, E., & Nikolskiy, P. (2017). Revising the archaeological record of the Upper Pleistocene Arctic Siberia: Human dispersal and adaptations in MIS 3 and 2. *Quaternary Science Reviews*, 165, 127–148.
- Plaskett, D. C. (1976). *Preliminary report: A Cultural resources survey in an area of the Nenana and Teklanika rivers of central Alaska*. Unpublished manuscript.
- Potter, Ben A., Irish, J. D., Reuther, J. D., Gelvin-Reymiller, C., & Holliday, V. T. (2011). A terminal Pleistocene child cremation and residential structure from eastern Beringia. *Science*, 331(6020), 1058–1062.
- Potter, B. A. (2008). Radiocarbon chronology of central Alaska: Technological continuity and economic change. *Radiocarbon*, 50(2), 181–204.
- Potter, B. A., Holmes, C. E., & Yesner, D. R. (2013). Technology and economy among the earliest prehistoric foragers in Interior Eastern Beringia. In Graf, K. E., Waters, M. R., & Ketron, C. V. (Eds.), *Paleoamerican Odyssey* (pp. 81–103). College Station, TX: Center for the Study of the First Americans.
- Potter, B. A., Ruether, J. D., Holliday, V. T., Holmes, C. E., Miller, D. S., & Schmuck, N. (2017). Early colonization of Beringia and North America: Chronology, routes, and adaptive strategies. *Quaternary International*, 444, 36–55.
- Powers, W. R., Guthrie, R. D., & Hoffecker, J. F. (2017). In Goebel, T. (Ed.), *Dry Creek: Archaeology and Paleoecology of a Late Pleistocene Alaskan Hunting Camp*. College Station, TX: Texas A&M University Press.
- Powers, W. R., & Hoffecker, J. F. (1989). Late Pleistocene settlement in the Nenana valley, central Alaska. *American Antiquity*, 54(2), 263–287.
- Puckett, N. N., & Graf, K. E. (in review). Chapter 3: Understanding space at Owl Ridge, central Alaska: Identifying activities and camp use. In K. Carlson and L. Bement (Eds.), *Diversity in Open Air Site Structure across the Pleistocene/Holocene Boundary* (18pp.). Boulder, CO, University of Colorado Press.
- Raghavan, M., Skoglund, P., Graf, K. E., Metspalu, M., Albrechtsen, A., Moltke, I., ... Willerslev, E. (2014). Upper Paleolithic Siberian genome reveals dual ancestry of Native Americans. *Nature*, 505, 87–91.
- Reimer, P. J., Bard, E., Bayliss, E., Beck, J. W., Blackwell, P. G., Bronk Ramsey, C., ... van der Plicht, J. (2013). Intcal13 and Marine13 radiocarbon age calibration curves 0–50,000 years cal yr BP. *Radiocarbon*, 55, 1869–1887.
- Ritter, D. F. (1982). Complex river terrace development in the Nenana Valley near Healy, Alaska. *Geological Society of America Bulletin*, 93(4), 346–356.
- Schweger, C. (1985). Geoarchaeology of northern regions: Lessons from cryoturbation at Onion Portage, Alaska. In J. K. Stein, & W. R. Farrand (Eds.), *Archaeological sediments in context* (pp. 127–141). Orono, ME: Center for the Study of Early Man, University of Maine.
- Schweger, C. E., Matthews, J. V., Jr., Hopkins, D. M., & Young, S. B. (1982). Paleoecology of Beringia—A synthesis. In Hopkins, D. M., Matthews, J. V., Jr., Schweger, C. E., & Young, S. B. (Eds.), *Paleoecology of Beringia* (pp. 425–444). New York, NY: Academic Press.
- Stuiver, M., & Polach, H. A. (1977). Discussion: Reporting of ^{14}C data. *Radiocarbon*, 19, 355–363.
- Thorson, R. M. (1986). Late Cenozoic glaciation of the northern Nenana river valley. In K. M. Reed, & R. M. Thorson (Eds.), *Glaciation in Alaska- The Geologic Record* (pp. 171–192). Anchorage, AK: Alaska Geological Society.
- Thorson, R. M., & Hamilton, T. (1977). Geology of the Dry Creek site; A stratified early man site in interior Alaska. *Quaternary Research*, 7(2), 149–176.
- Tinner, W., Hu, F. S., Beer, R., Kaltenrieder, P., Scheuer, B., & Krahenbuhl, U. (2006). Postglacial vegetational and fire history: pollen plant microfossil and charcoal records from two Alaskan lakes. *Vegetation History and Archaeobotany*, 15, 279–293.
- Ward, G. K., & Wilson, S. R. (1978). Procedures for comparing and combining radiocarbon age determinations: A critique. *Archaeometry*, 20(1), 19–31.
- Warhaftig, C. (1958). Quaternary geology of the Nenana River valley and adjacent of the Alaska Range. *U.S. Geological Survey Paper*, 293-A, 1–68.
- Waythomas, C. F., & Kaufman, D. S. (1991). Comment on: "Latest Pleistocene Increase in Wind Intensity Recorded in Eolian Sediments from Central Alaska," by N. Bigelow, J. E. Beget, and W. R. Powers. *Quaternary Research*, 36, 329–333.
- West, F. H. (1967). The Donnelly Ridge site and the definition of an early core and blade complex in central Alaska. *American Antiquity*, 32(3), 360–382.

- Wood, W. R., & Johnson, D. L. (1978). A survey of disturbance processes in archaeological site formation. In M. B. Schiffer (Ed.), *Advances in archaeological method and theory* (Vol.1, pp. 315–381). New York, NY: Academic Press.
- Wygall, B. T. (2018). The peopling of eastern Beringia and its archaeological complexities. *Quaternary International*, 466(Part B), 284–298.
- Younie, A. M., & Gillispie, T. E. (2016). Lithic technology at Linda's point, Healy Lake, Alaska. *Arctic*, 69(1), 79–98.

How to cite this article: Graf KE, Gore AK, Melton JA, et al. Recent excavations at Owl Ridge, interior Alaska: Site stratigraphy, chronology, and site formation and implications for late Pleistocene archaeology and peopling of eastern Beringia. *Geoarchaeology*. 2019;1–24.
<https://doi.org/10.1002/gea.21754>